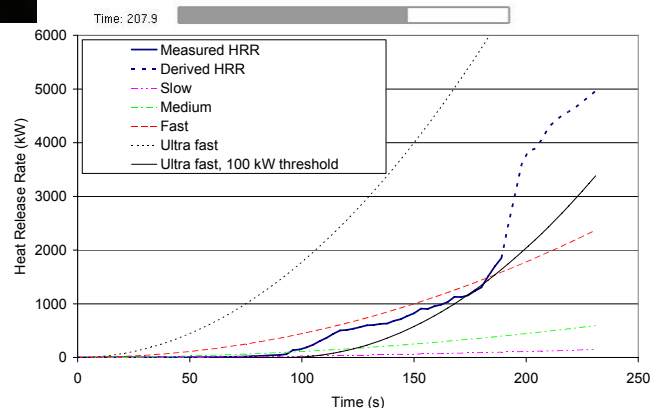
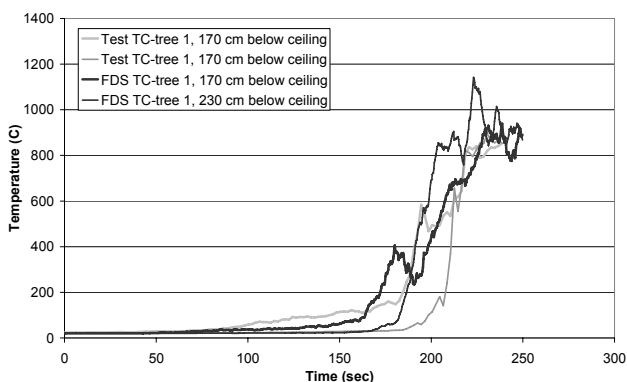
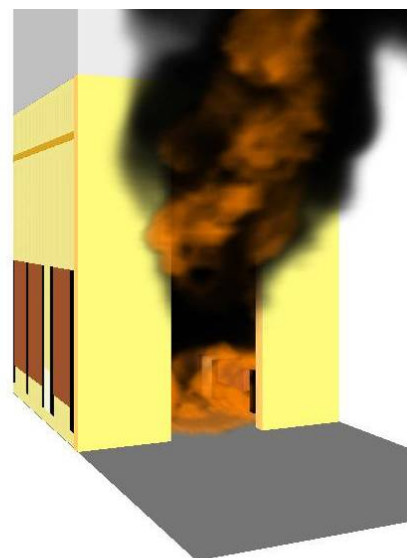


Design fire for a train compartment

Maria Hjohlman, Michael Försth, Jesper Axelsson

SP Technical Research Institute of Sweden



Brandforsk project 401-051

Design fire for a train compartment

Maria Hjohlman, Michael Försth, Jesper Axelsson

Brandforsk project 401-051

Abstract

Design fire for a train compartment

The fire dynamics of a train compartment was investigated in detail. A full scale test was performed which showed that the compartment reached flashover three minutes after ignition. Small scale tests were performed on the wall and floor linings and on seat and table materials. The results from these tests were used as input to a CFD-model implemented in FDS5 (Fire Dynamics Simulator, v5). It was possible to obtain a good correlation between the FDS5 model and the full scale experiment. However, in order to obtain this correlation it was necessary to deviate significantly from the small scale experimental results regarding the thermal conductivity of the seat material. Further, the FDS5 model was highly sensitive to grid size.

Despite these drawbacks it was concluded that FDS5 can be used to determine design fires for the tested compartment and for geometries and material selections which do not differ drastically from the tested configuration. A much simpler way to obtain a design fire is to use so called t^2 pre-flashover fires. Using this approach it was found that the growth rate of the compartment fire was between fast and ultra fast, with characteristic time scales of 150 s and 75 s, respectively. Finally it was concluded that the main part of the heat release originated from the seats and that a reasonable good design fire can be found by studying the fire dynamics of individual seats only.

Key words: design fire, train, material properties, small scale, large scale, field modeling, FDS, seat

SP Sveriges Tekniska Forskningsinstitut
SP Technical Research Institute of Sweden

SP Report 2009:08
ISBN 978-91-85829-79-8
ISSN 0284-5172
Borås 2009

Contents

Preface	6
Summary	7
Sammanfattning	9
Abbreviations	11
1 Introduction	12
2 Full scale fire test of a train compartment	15
2.1 Train compartment	15
2.1.1 Origin of train compartment	15
2.1.2 Dimensions, surface linings and equipment	16
2.2 Fire test	17
2.2.1 Detectors and measurements	17
2.2.2 Ignition source	21
2.2.3 Results	22
3 Material data	28
3.1 Full scale tests of seat	28
3.1.1 Free-burning in the furniture calorimeter	28
3.1.2 Test in ISO 9705 room	31
3.1.3 Results	33
3.2 Small scale tests of seat, table, and lining materials	33
3.2.1 Experimental setup	33
3.3 Ignition temperatures and thermal properties	34
3.3.1 Results and analysis	35
4 Standardized design fires – Pre-flashover t^2 fires	41
5 Design fires by analytical methods – Superpositioning of HRR curves	43
5.1 Example 1	43
5.2 Example 2	44
5.3 Example 3	45
6 Design fires by CFD field modelling – FDS5	47
6.1 Model	47
6.1.1 Geometry	47
6.1.2 Material properties	48
6.2 Results	49
6.2.1 Grid size dependency	53
7 Other methods	55
7.1 Two-zone models	55
7.2 ConeTools	55
8 Discussions and conclusions	56
Appendix A: Radiation measurements from the full scale test	58

Appendix B: Data from the Small scale tests of seat, table, and lining materials	59
8.1 Seat material	60
8.1.1 Products	60
8.1.2 Test specification	60
8.1.3 Test results	60
8.1.4 Graphs of heat release rate and smoke production rate	61
8.1.5 Measured data	62
8.1.6 Conditioning	62
8.1.7 Date of test	62
8.2 Metal laminate	63
8.2.1 Products	63
8.2.2 Test specification	63
8.2.3 Test results	63
8.2.4 Graphs of heat release rate and smoke production rate	64
8.2.5 Measured data	65
8.2.6 Conditioning	65
8.2.7 Date of test	65
8.3 HPL laminate	66
8.3.1 Products	66
8.3.2 Test specification	66
8.3.3 Test results	66
8.3.4 Graphs of heat release rate and smoke production rate	67
8.3.5 Measured data	68
8.3.6 Conditioning	68
8.3.7 Date of test	68
8.4 PVC-carpet	69
8.4.1 Products	69
8.4.2 Test specification	69
8.4.3 Test results	69
8.4.4 Graphs of heat release rate and smoke production rate	70
8.4.5 Measured data	71
8.4.6 Conditioning	71
8.4.7 Date of test	71
8.5 Wood table	72
8.5.1 Products	72
8.5.2 Test specification	72
8.5.3 Test results	72
8.5.4 Graphs of heat release rate and smoke production rate	73
8.5.5 Measured data	74
8.5.6 Conditioning	74
8.5.7 Date of test	74
8.6 Test results explanation – ISO 5660	75
References	76

Preface

The Swedish Board for Fire Research (Brandforsk) sponsored this project with reference number 401-051 which is gratefully acknowledged. Brandforsk is owned by the Swedish government, insurance companies, local authorities and industry and has as its mission to initiate, finance and follow-up different types of fire research.

Acknowledgements are given to the staff at SP who has contributed to this project. Special thanks to Magnus Samuelsson, Lars Pettersson and Hans Boström.

Summary

In this report design fires for trains, buses and similar vehicles have been studied. The focus has been on pre-flashover design fires which are used for design of egress capacities and fire protection. Three different methods for determining design fires were employed. In order to develop, validate and compare the different methods, a full scale experiment was performed on a train compartment which was used as a test case and reference scenario. In addition extensive small scale experiments were performed in order to obtain material properties needed for two of the methods for determining design fire.

The first method is based on ISO/TR 13387 where pre flashover t^2 design fires are formulated. No material properties are needed for this method and it is simply assumed that the fire grows quadratically with time. The only free parameter is the characteristic time scale which gives a measure of the growth rate. It was found that a “fast” growth rate, with a characteristic time scale of 150 s, best reproduced the heat release rate (HRR) from the full scale experiment until the time of flashover. After flashover the HRR was vastly underestimated using a fast t^2 design fire. This method is very simple to use since no small scale experiments are needed. However, its validity for enclosures that differ considerably from the train compartment tested in this study cannot be confirmed.

The second method used was to superposition the HRR contributions found in the small scale experiments. This can be done by scaling of the data, thus compensating for the difference in exposed areas in the small scale and the full scale experiments. Reasonable design fires could be obtained in this way, although they were conservative in the pre-flashover phase. After flashover this method is less useful since it does not take into account phenomena such as oxygen depletion and high irradiation levels.

The third method was the computationally most sophisticated one. A field model implemented in the software FDS5 (Fire Dynamics Simulator, version 5) was employed. This method makes full use of the results from the small scale experimental data such as HRR, ignition temperatures and thermal conductivities. It was possible to reproduce the HRR fairly well with this method, to a certain degree even after flashover. However, this was done at the expense of generality of the method since one material parameter, the conductivity of the seat, had to be adjusted to a different value than the one obtained in the small scale test in order to obtain flame spread in agreement with the full scale experiment. All other material parameters were set to the same value as that found experimentally. Another lack of generality was that the model was highly sensitive to grid size. The agreement with full scale experimental data was obtained using a grid size of 5 cm. Other grid sizes produce results that deviate considerably from the experimental data. This means that the model has only been strictly validated for geometries similar to the one tested in the full scale experiment.

In brief, it has been found that all three methods are useful if the compartment studied does not deviate considerably from the one studied here. The method of choice would then be to use a pre-flashover t^2 curve with a characteristic time scale of 150 s since this is the simplest method. If the type of compartment is considerably different, such as a train saloon, bus, or tram for example, it seems appropriate to use the superposition method where the HRR curves of the different individual materials are summarized. Finally, if post-flashover HRR information is needed FDS5 seems to be the only suitable choice since this method takes, for example, oxygen depletion and high irradiation levels into consideration, which is not the case for the other methods. If the compartment is similar to the compartment tested in this study the confidence in the design fire obtained is relatively high. If the compartment is fundamentally different, any attempt to obtain a

design fire for post flashover conditions by performing small scale tests only is subject to significant uncertainties and new full-scale tests are advisable.

Sammanfattning

I detta projekt har dimensionerande bränder för tåg, bussar och liknande fordon studerats. Fokus har legat på dimensionerande bränder innan övertändning vilka används för dimensionering av till exempel brandskydd och utrymningsvägar. Tre olika metoder för att bestämma dimensionerande brand har använts. För att utveckla, validera och jämföra metoderna har ett fullskaleexperiment av en tåghytt genomförts som referensscenario. Som komplement till detta har flera småskaliga prov utförts för att bestämma de materialparametrar som behövs för två av de föreslagna metoderna.

Den första metoden bygger på standarden ISO/TR 13388 och använder sig av så kallade t^2 dimensionerande bränder för tiden fram till övertändning. Inga materialparametrar är nödvändiga och man antar helt enkelt att branden växer kvadratisk med tiden. Den enda fria parametern är en karakteristisk tidsskala som bestämmer hur snabbt branden växer till. Studien visade att en så kallad snabb brandtillväxt, med en karakteristisk tidsskala om 150 s, ger bäst överensstämmelse med fullskaleförsöken fram till övertändning. Efter övertändning underskattades värmeeffekten dramatiskt med t^2 kurvan jämfört med fullskaleexperimentet. Metoden är mycket enkel att använda eftersom inga småskaliga försök är nödvändiga. Däremot är metodens giltighet osäker vad gäller utrymmen som betydligt skiljer sig från tågkupén som testades i fullskaleförsöket.

Den andra metoden var att addera värmeeffektskurvor från de olika materialen i tågkupén. Detta kan göras genom att utgå från de värmeeffekter som uppmätts i småskaleförsöken och sedan kompensera för att större ytor exponeras i fullskaleexperimentet jämfört med i småskaleförsöken. En rimlig överensstämmelse med fullskaleexperimenten kunde erhållas på detta sätt. De dimensionerande bränderna blev dock generellt konservativa, dvs. högre än motsvarande resultat från fullskaleförsöken, fram till tidpunkten för övertändning. Efter övertändning är denna metod mindre användbar eftersom den inte kan ta hänsyn till effekter som syrereduktion och höga strålningsnivåer som förekommer efter övertändning.

Den tredje metoden var den beräkningstekniskt mest avancerade. En fältmodell implementerad i mjukvaran FDS5 (Fire Dynamics Simulator, version 5) användes. Denna metod använder alla resultat från de småskaliga försöken såsom värmeeffekt, antändningstemperatur och termisk ledningsförmåga. Det var möjligt att reproducera den fullskaliga värmeeffektskurvan, till viss del även efter övertändning. Däremot är det problematiskt att generalisera denna modell till andra geometrier och materialval eftersom en materialparameter, den termiska ledningsförmågan hos sätet, justerades till ett annat värde än det som erhållits i småskaleförsöket. Detta var nödvändigt för att få en flamspridning i modellen som överensstämde med den i fullskaleförsöket. Alla andra materialparametrar var dock identiska med resultaten från småskaleförsöken. Ett annat problem med FDS-modellen var att den är mycket känsligt för cellstorleken i den numeriska griden. Genom att använda cellstorlek 5 cm erhålls överensstämmelse med fullskaleförsöken men för andra cellstorlekar erhålls betydligt avvikande resultat. Detta betyder att modellen endast är strikt validerad för geometrier och material liknande de som testades i fullskaleförsöket.

Sammanfattningsvis kan sägas att alla tre metoder är användbara om utrymmet inte avviker alltför mycket från den tågkupé som undersökts i fullskaleförsöket. Det är då enklast att använda en dimensionerande brand enligt en t^2 kurva med en karakteristisk tidsskala om 150 s. Om utrymmet skiljer sig markant från tågkupén i fullskaleförsöket är det lämpligt att använda metoden med att addera värmeeffektskurvor som erhållits från småskaleförsöken. Slutligen, om en dimensionerande brand för tiden efter övertändning önskas är FDS5 lämpligt att använda eftersom metoden tar hänsyn till faktorer såsom

syreproduktion och de höga strålningsnivåer som förekommer efter övertändning. Om utrymmet markant skiljer sig från den kupé som provades i fullskaleförsöket så är det svårt att endast med hjälp av småskaleförsök beräkna en dimensionerande brand efter övertändning. Det är då lämpligt att utföra nya fullskaleförsök.

Abbreviations

α_s	surface absorptivity [-],
\dot{q}_{cr}	critical irradiation level for ignition [kWm^{-2}],
\dot{q}_{min}	minimum irradiation level for ignition [kWm^{-2}].
h_c	convective coefficient [$\text{kWm}^{-2}\text{K}^{-1}$]
T_{ign}	ignition temperature [$^{\circ}\text{C}$],
T_{∞}	ambient temperature [$^{\circ}\text{C}$],
σ	Stefan-Boltzmann constant, $\sigma=5.67 \cdot 10^{-11} \text{ kWm}^{-2}\text{K}^{-4}$,
\dot{q}	irradiation level [kW/m^2],
K	thermal conductivity [$\text{Wm}^{-1}\text{K}^{-1}$],
ρ	density [kgm^{-3}],
C	specific heat [$\text{JK}^{-1}\text{kg}^{-1}$],
t_{ign}	time to ignition [s],
T_0	initial temperature [$^{\circ}\text{C}$].

1 Introduction

A design fire describes a possible outcome of a specific fire scenario. In *ISO/TS 16733, Fire Safety Engineering – Selection of Design Fire Scenarios and Design Fires* [1] a design fire is defined as

“a quantitative description of assumed fire characteristics within a Design Fire Scenario. Typically, an idealised description of the variation with time of important fire variables such as heat release rate and toxic species yields, along with other important input data for modelling such as the fire load density.”

In fire safety engineering analysis today, different design fire scenarios are evaluated using the design fire as the design factor. The design fire can be used for designing, for example, egress capacities, fire protection systems or construction of building components. In this report the design fire studied is the heat release rate (HRR) from a fire started from a vandalized passenger seat in a train compartment. The time span considered is from ignition to flashover. Flashover means that the air flow into the compartment can no longer sustain the fire and uncombusted gases therefore exit the door, resulting in large flames protruding into neighbouring volumes. Such a design fire is useful for estimating the time for egress and the dynamics of fire spread to the rest of the train, or the vehicle in question. Another type of design fire for vehicles, not considered in this report, is the fire load from a vehicle consumed by flames. Such a design fire is of less use for the analysis of egress and fire spread inside the vehicle but is of great interest for the design of, for example, tunnels.

The general purpose of this project was to establish efficient methods for determining appropriate design fires for trains, buses, and similar vehicles based on limited small-scale testing. A train compartment was used as a test case where the investigated methods could be compared with the results from a full-scale experiment.

Data from real tests are extremely valuable in the process of selecting a design fire, either to be used directly as a representative fire or for comparison reasons to justify the selection of the curve or curves. However, available data from full scale tests of trains or busses are very limited. A summary of some important work in this field that has generated valuable data is provided below.

In the EUREKA-project FIRETUNE [2], the fire behaviour of seven railway and subway cars and one bus was tested in the Repparfjord Tunnel in Norway, 1991-1992. The cars, representing different types, constructions and interior materials, are relatively well documented in the report. The tests are conducted inside the tunnel with the aim to study the fire growth and fully developed fire of the vehicles in a tunnel environment. Since each test starts with a fire source inside the passenger compartments of the cars and the enclosure is heavily instrumented, the tests also provide some valuable information about the incipient, growing and fully developed phase of the fire inside the passenger compartments. Temperature distribution inside the car compartment, CO and CO₂ concentration and optical density in the tunnel, were measured and observations during the tests, such as flame spread, smoke distribution and breakage of windows, were made. Not all test results include information about HRR but for some tests estimations of the HRR curve, based on enthalpy flow, O₂ consumption and CO and CO₂ concentrations, were made. Ingasson and Lönnemark (2004) [3] draw the conclusion from the test series that the parameters having greatest influence on the fire development in the railway och subway cars can be ranked as follows:

1. Fire behaviour of the windows and how they are attached to the window frames.

2. Fire behaviour of the lining material (wall, ceiling and floor) and seats, their fire load and how they are positioned in the car compartment.
3. Type of construction of the railway and subway car (steel or aluminium).
4. Size and position of fire source.
5. Door openings and possible ceiling openings.
6. Moisture content of the material.
7. Possible luggage.

In the EU-project FIRESTARR, several real scale fire tests on widely used wall and ceiling lining materials were tested in a compartment with the size and ventilation conditions of an SNCF Voiture VU78 railway carriage [4]. The fire source was a propane burner which has been designed to simulate the heat output and heat flux on the compartment walls caused by a typical burning vandalised railway seat. A total of 12 products were tested, of which 6 products caused the room to go to flashover conditions in 194 to 420 seconds.

In the same project, 8 seats assembled on typical frames, insulation and linear products for seat of passenger trains, were tested as well. Each of the three main components of the seats had been exposed to the small scale tests, e.g., the cone calorimeter test ISO 5660 (35 and 50 kW/m²). The seats were tested, two or three in each test, in the same compartment as described above. Heat release rates and observations, such as whether the second or third seat ignited, were documented.

CSIRO Fire Science and Technology Laboratory (Australia) presented the results of a large-scale fire test of a complete Australian suburban passenger train carriage at the 8th symposium of Fire Safety Science, 2005 [5]. The test was conducted in the open, not in a tunnel, and no attempts to calculate or estimate the heat release were presented. During the tests, measurements of temperature, gas flow, heat flux and gas composition, were conducted inside the carriage. The fully developed fire went to flashover at 140 s after ignition. It was concluded that the ceiling and upper wall linings are more critical for fire spread than the seats and lower wall linings.

In USA several fire tests in a passenger rail coach were conducted in 1999 by NIST [6]. Different fire sources were used on or below passenger seats as well as in a corner of the rail car. For all but one test the flame spread and damage was limited to the area in the close vicinity of the burner. It was concluded that a fire source of more than 25 kW was necessary to promote significant fire spread. In one test there was extensive flame spread to adjacent seats, table wall lining and luggage rack before the test was terminated to allow additional tests to be conducted in the rail car. Temperatures, gas concentrations, heat flux, smoke obscuration and heat release rate measurements, were conducted during the tests.

The large-scale fire tests were conducted as phase three of an extensive project about fire hazard analysis of passenger trains. Phase one [7] consisted of small scale reaction to fire tests of interior materials in passenger rail cars, including comparisons between the different methods used. Phase two [8] incorporated measurements of fire performance of real-scale furnishings and lining materials using a furniture calorimeter, and discussions about determining available egress times for rail car passengers in case of fire using mathematical modelling. Examples using the CFAST zone model to calculate the temperature and smoke distribution in the passenger compartment for different rail car designs were presented in the report. The design fire curves used in the examples were the t^2 design curves described in ISO/TR 13387-2 [9] and in Section 4 of this report, HRR curves from the real-scale furnishing tests conducted in the same phase of the project and a fictive HRR curve based on the HRR curves obtained in tests and the conservative assumption that all material ignites simultaneously.

The present report contains suggestions for methods to determine appropriate design fires for trains and for similarly configured vehicles such as buses, trams and large cars. The methods are compared to each other at the end of the report and the analysis is supported by extensive experimental data. Section 2 contains a description of the train compartment selected as a case study in this report, as well as experimental results from a full-scale fire test. These results are needed for validation of the methods presented in Section 4 to Section 6 for determining design fires. Further, this full-scale test is by itself of value as a data source for a well-defined fire in a train compartment. Section 3 contains the results from small-scale tests on seats, wall and floor linings, and the wooden table that was placed in the compartment. These results are needed to enable the use of two of the methods for determining an appropriate design fire (Section 5, superposition of HRR curves and Section 6, field modeling using FDS5). Section 4 presents one of the simplest ways of prescribing a design fire. It is assumed that the fire grows quadratically with time. No small-scale experimental data are needed for this method. In Section 5 design fires are developed based on the addition of HRR curves obtained from the small-scale experiments. Section 6 contains the most sophisticated method where field-modelling, implemented in the software FDS5, is used to predict the outcome of the compartment fire. This method takes flame spread, oxygen depletion, radiation and many other factors into consideration. The method requires the results from the small scale experiment as input parameters. Section 7 shortly discusses some alternative methods for determining design fires, not used in this project. A discussion and comparison of the methods is presented in Section 8.

2 Full scale fire test of a train compartment

The full scale experiment was performed on a train compartment of size 196 cm × 200 cm. Size and budget constraints were the factors behind the decision to investigate a single compartment and not an entire train car. The purpose of the project was to elaborate on methods for how a design fire for an arbitrary space can be developed, using small scale experiments and various computational tools with different degrees of sophistication. For this purpose the selection of a well-defined compartment is well motivated.

2.1 Train compartment

2.1.1 Origin of train compartment

The compartment investigated in the full-scale test originates from a BF4 car [10] build by Kalmar Verkstads AB 1985 and 1986. The exterior of the car is shown in Figure 1 while an overview of the interior is shown in Figure 2. As can be seen the car is divided into a goods section and a passenger section. The passenger section consists of a saloon and a passenger compartment (or “box”), indicated by the arrow in Figure 2.



Figure 1 Exterior of the BF4 car. This is the car type that contains the compartment investigated in this study [10].

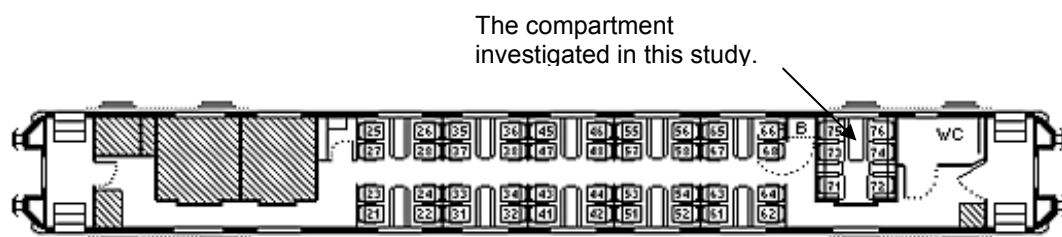


Figure 2 Overview of the car investigated in this study [10].

Figure 3 shows a photo of the interior of the train compartment investigated in this study.



Figure 3 Interior from a compartment of the type investigated in this study [10].

2.1.2 Dimensions, surface linings and equipment

The dimensions of the compartment are indicated in Figure 7. The height of the compartment was 2.4 m and the height of the door was 2.0 m. The composition of the compartment is given in Table 1 below, see also Figure 4.

Table 1 Composition of the train compartement used in the full scale test.

Seats	Two double seats and two single seats made of fabric on PUR-foam. The weight of a double seat was 196 kg.
Tables	Three wooden tables. The large table, seen in Figure 3, weighed 12 kg and the small tables, seen in Figure 4, weighed 3 kg each.
Window	The window was simulated with an non-combustible Promatect board
Luggage rack	Two luggage racks made of wood and plastic, see Figure 3. Each luggage rack weighed 25 kg.
Floor	PVC-carpet. Thickness 2 mm. Density 1400 kg/m ³ .
Ceiling	Non-combustible plasterboard
Wall – long sides	HPL laminate glued on plywood. Thickness 20 mm. Density 548 kg/m ³ .
Wall – short sides	Metal laminate glued on plywood. Thickness 20 mm. Density 648 kg/m ³ .

Since the window was simulated with an non-combustible Promatect board, this test does not account for breaking or falling out of the window. This has limited importance for the early pre-flashover phase, but may be significant if the fire develops and becomes ventilation controlled.

2.2 Fire test

2.2.1 Detectors and measurements

The train compartment was heavily equipped with detectors in order to characterize the fire as exactly as possible. Three thermocouple trees were placed at different positions in the compartment, the positions of the thermocouple trees and the individual thermocouples are shown in Figure 4, Figure 5, and Figure 7.

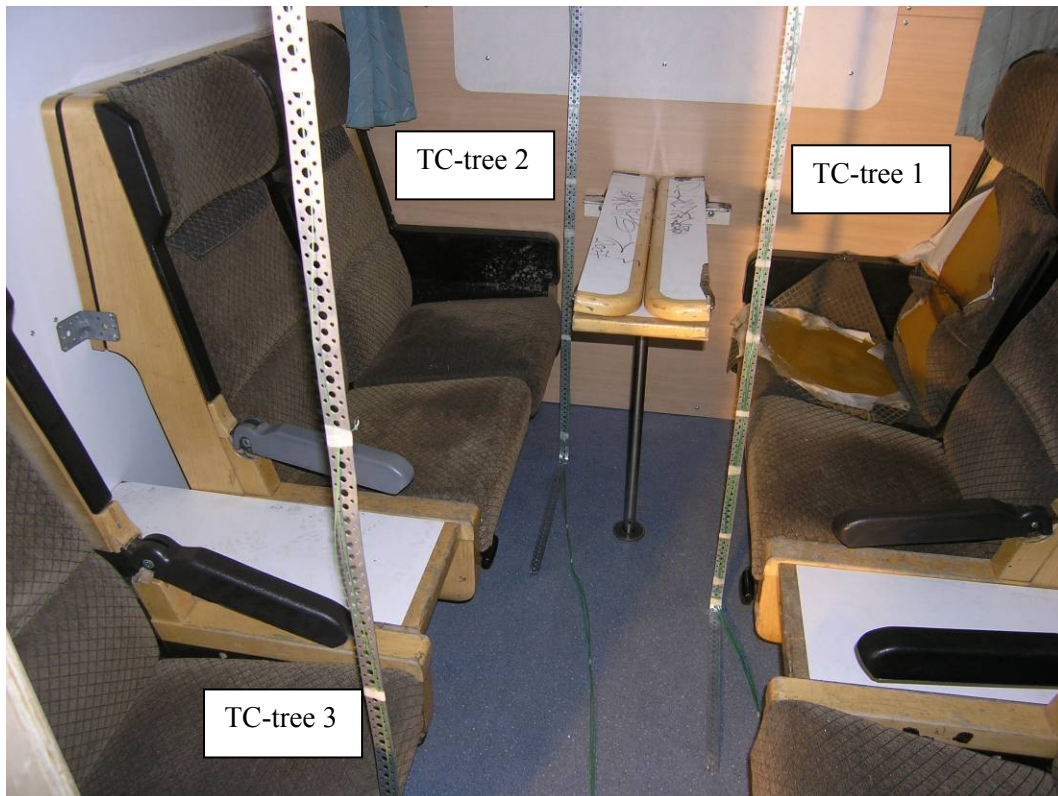


Figure 4 Position of the thermocouple trees in the compartment. The distances from the ceiling of the different thermocouples are indicated in Figure 5

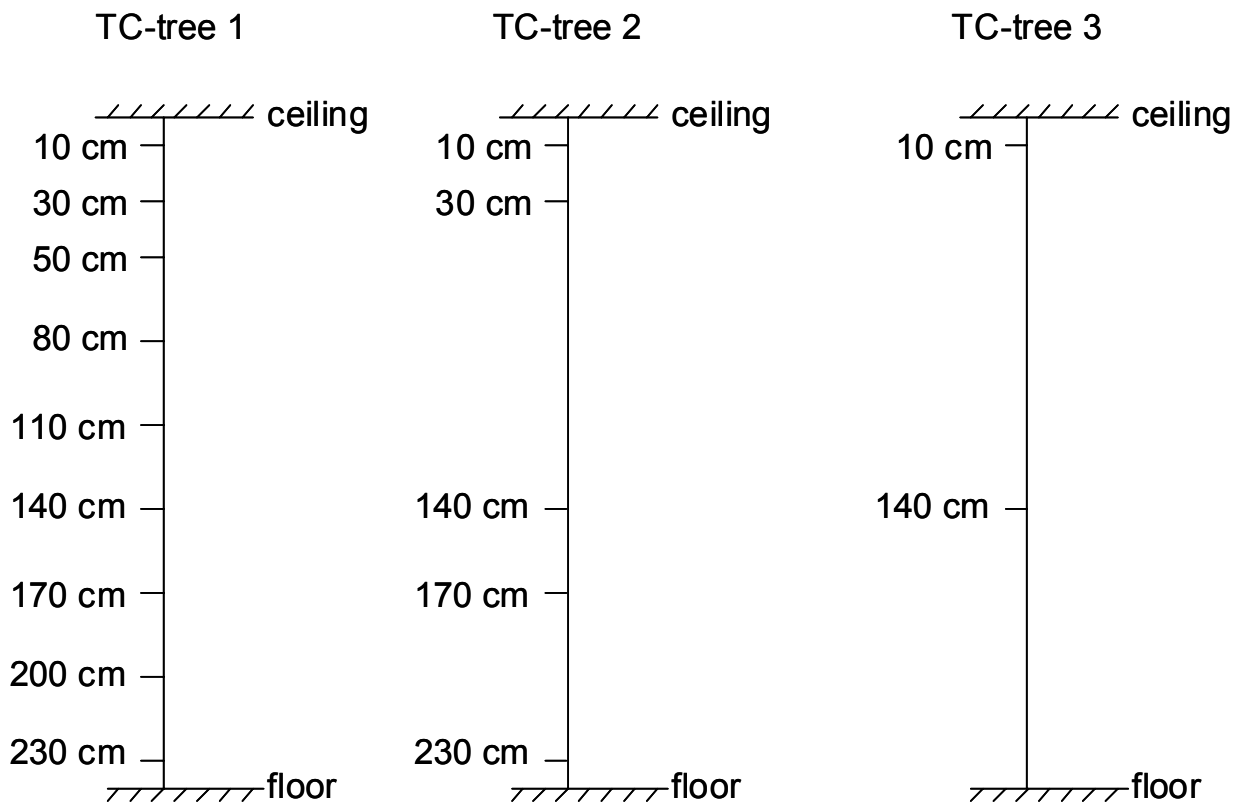


Figure 5 Distances from the ceiling for the different thermocouples.

Radiation was measured with two Schmidt-Boelter type instruments, Medtherm 64-1-18 and Medtherm 64-2-18, and two plate thermometers [11]. The positions of the radiation detectors are shown in Figure 6 and Figure 7. Radiation results are presented in Appendix A.

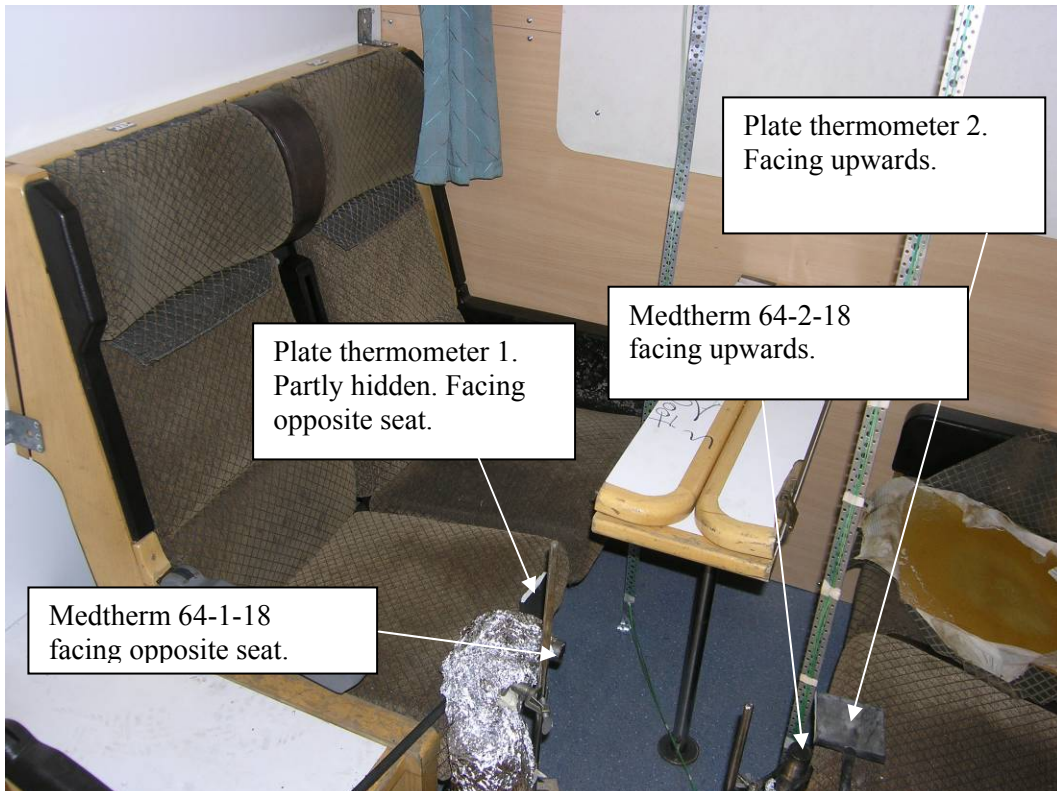


Figure 6 Position of the four radiation detectors.

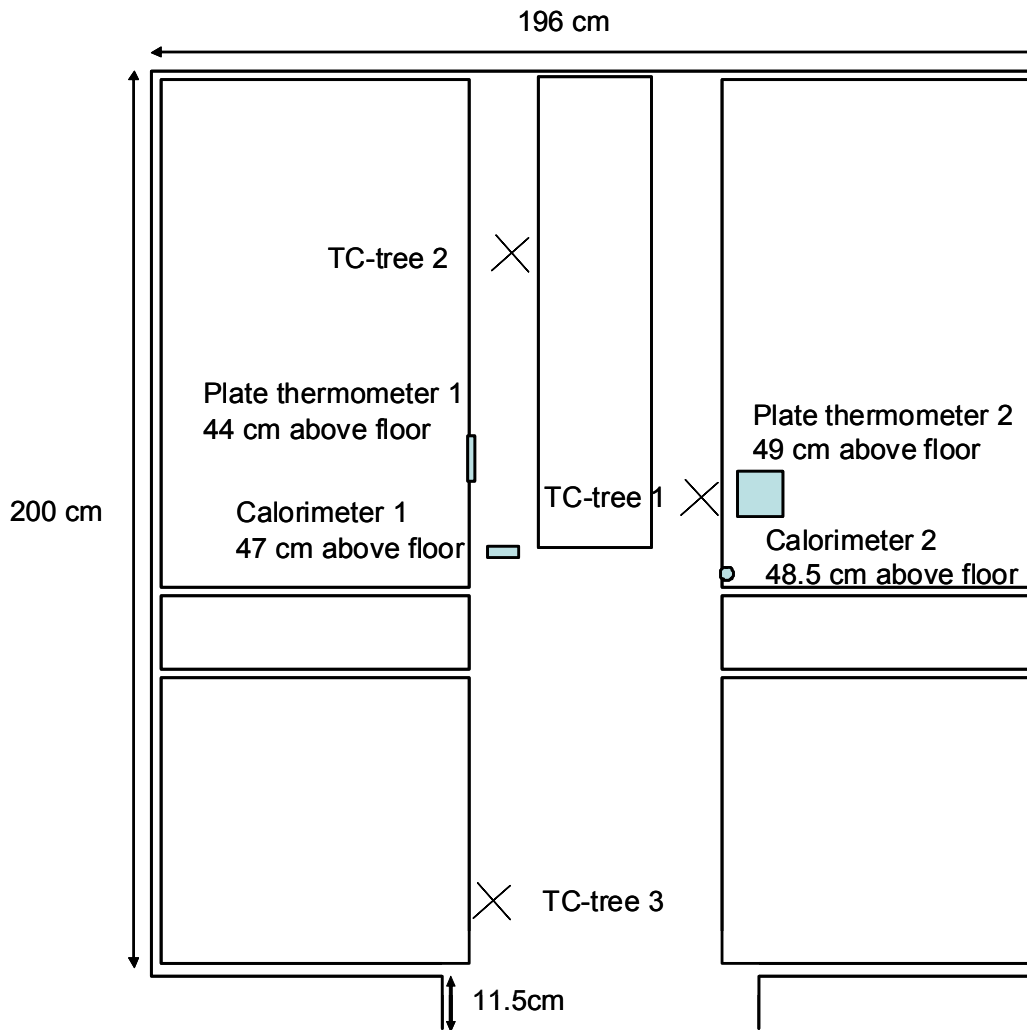


Figure 7 Geometry of the compartment and furniture with positions of the TC-trees and radiation detectors.

Heat release rate was measured using the setup of the ISO 9705 test standard [12], see Figure 8. The smoke gases coming out from the room were collected by a hood and exhaust system from which samples were taken for gas analysis. In this experiment the ISO 9705 wall containing the door was completely removed and the train compartment was built in the inner right hand corner of the room, see Figure 9.

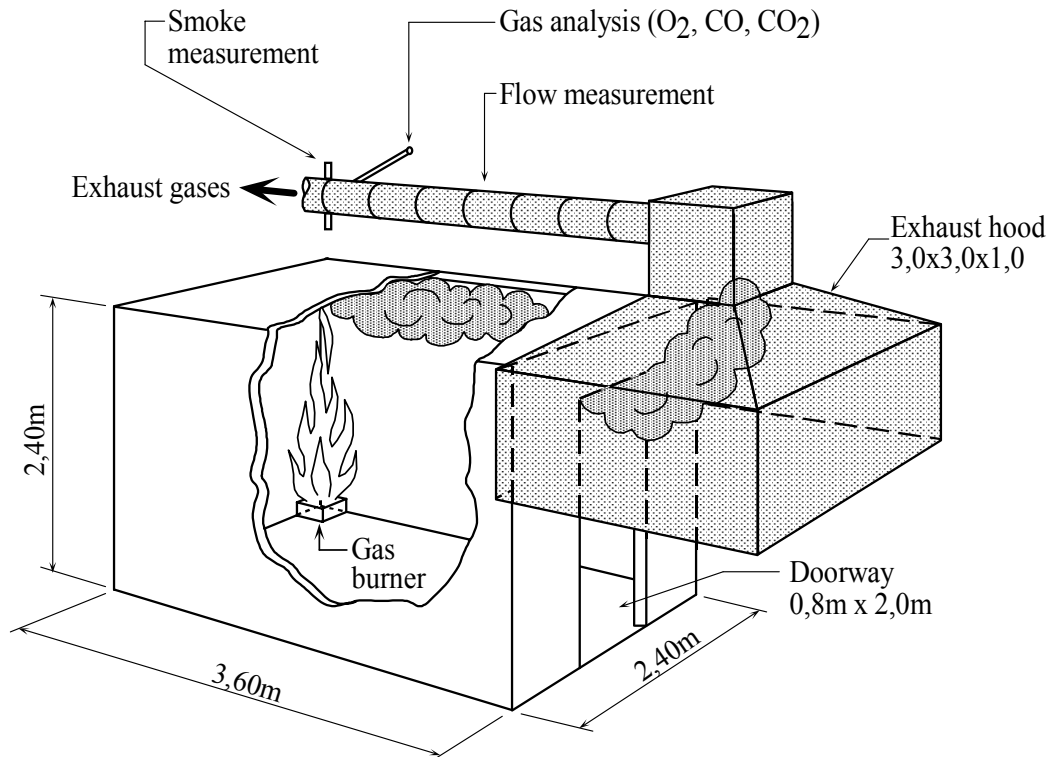


Figure 8 Schematic drawing of the original ISO 9705 room test equipment.



Figure 9 Photo illustrating how the train compartment was built in the inner right part of the modified ISO 9705 room.

2.2.2 Ignition source

The fire was initiated by igniting a seat with a 7 kW propane burner, see reference [13]. The outer dimensions of the square burner were 115 mm × 115 mm. The burner was positioned 10 mm from the backrest and 10 mm above the seat, see Figure 10 and Figure 11. The flame from the burner was applied to the seat in 76 seconds at which time it was removed from the compartment due to excessive heat.

The seat ignited by the burner was prepared according to the instructions in reference [13]. This means that it was vandalized in a standardized way. The vandalism together with the 7 kW propane burner simulates the course of action that can be expected from an arsonist.



Figure 10 The square burner used for igniting the seat. Also notice the standardized vandalism of the seat [13].



Figure 11 A few seconds after the square burner was ignited.

2.2.3 Results

Table 2 shows the most important observations during the test.

Table 2 List of important events that occurred during the test

Event	Time (mm:ss)
Ignition	00:00
Fire on back of ignited seat	00:20
Entire back of ignited seat in flames	01:00
Burner was removed	01:16
Flames from luggage rack	01:30
Entire ignited seat in flames	01:45
Fire in metal laminate on inner wall	02:00
Droplets from luggage rack	02:20
Entire seat neighbouring ignited seat in flames	02:30
Entire third seat in the right row (lower right seat in Figure 7) in flames	03:00
Entire left seat row ignited	03:00
Radiation detectors were removed	03:05
Flashover. Large flames exiting the compartment.	03:15
Extinction	03:50

The heat release rate is shown in Figure 12. The solid line shows measured data. Due to saturation of the gas analyzer for heat release rates above 1800 kW no HRR data was obtained using the oxygen depletion calorimetry after 180 s. However, the dashed curve is an estimation of the heat release based on temperature measurements in the exhaust gases. As can be seen the heat release increased rapidly and flashover occurred after only three minutes, see Table 2.

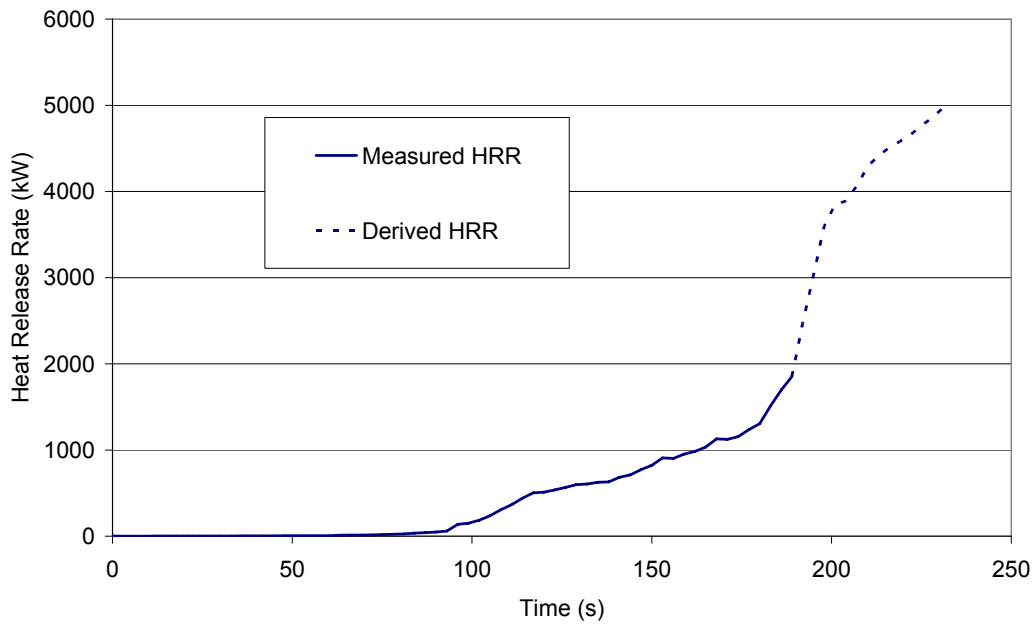


Figure 12 The heat release rate from the compartment fire as a function of time. The solid line corresponds to values measured using oxygen depletion calorimetry, the dashed line is an estimation of the heat release based on temperature measurements. The curve stops at 230 s when the fire was extinguished by water.

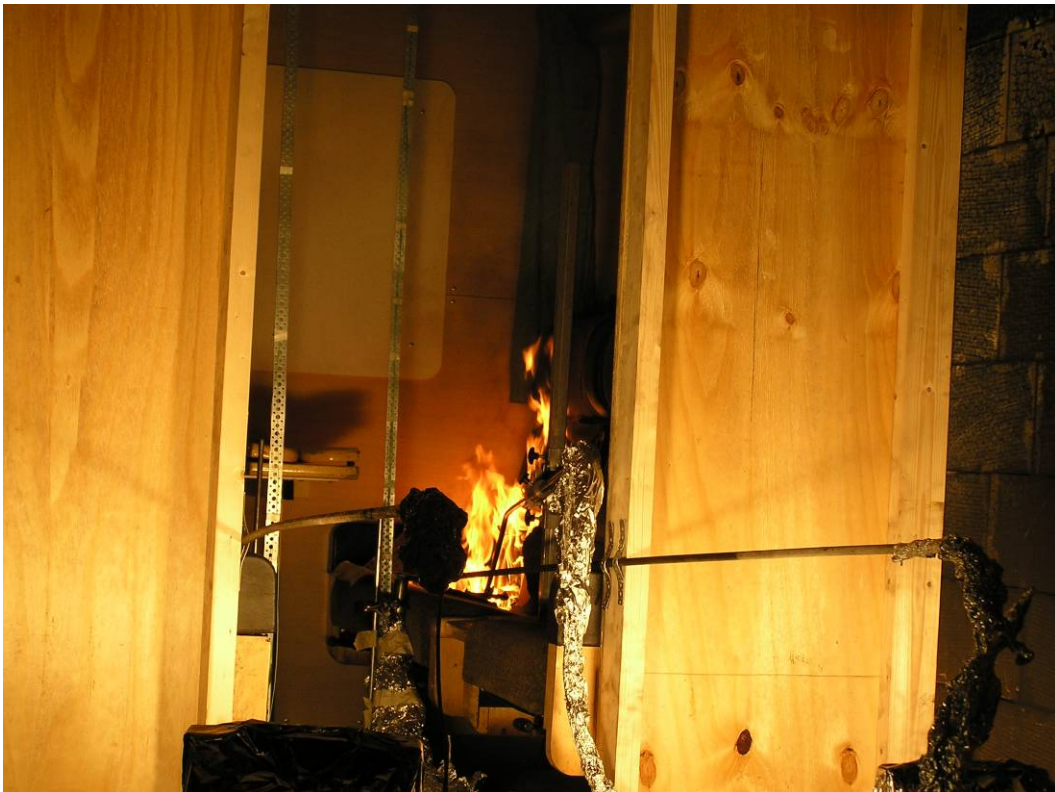


Figure 13 Fire development 54 s after ignition of the propane burner.



Figure 14 Fire development 132 s after ignition of the propane burner.



Figure 15 Fire development 208 s after ignition of the propane burner.



Figure 16 Fire development 218 s after ignition of the propane burner.

The measured temperatures are shown in Figure 17 to Figure 20 below. The temperatures for thermocouple tree 1 have been separated into two graphs for clarity.

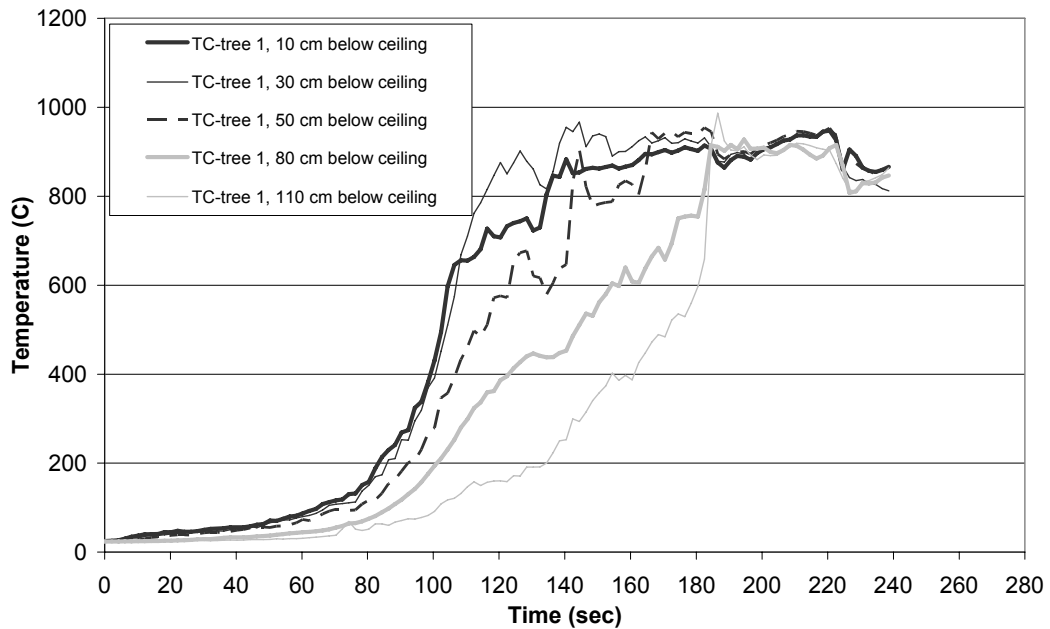


Figure 17 Measured temperatures in thermocouple tree 1 10-80 cm from the ceiling. The positions of the thermocouple trees are shown in Figure 7.

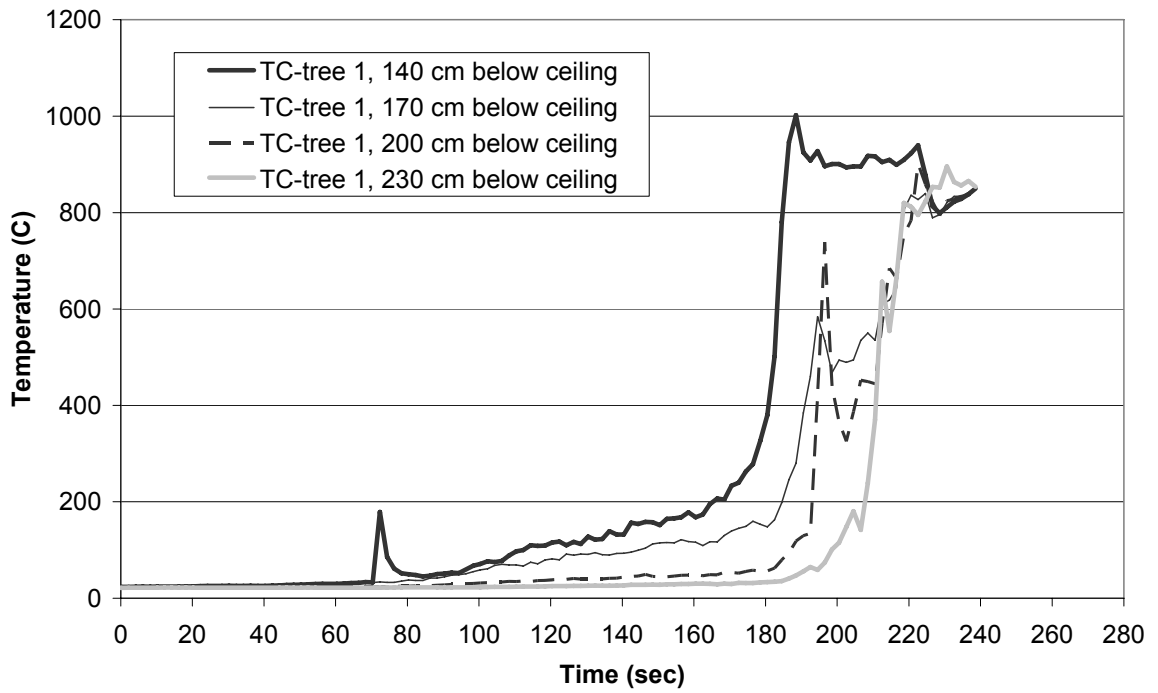


Figure 18 Measured temperatures in thermocouple tree 1 140-230 cm from the ceiling. The positions of the thermocouple trees are shown in Figure 7.

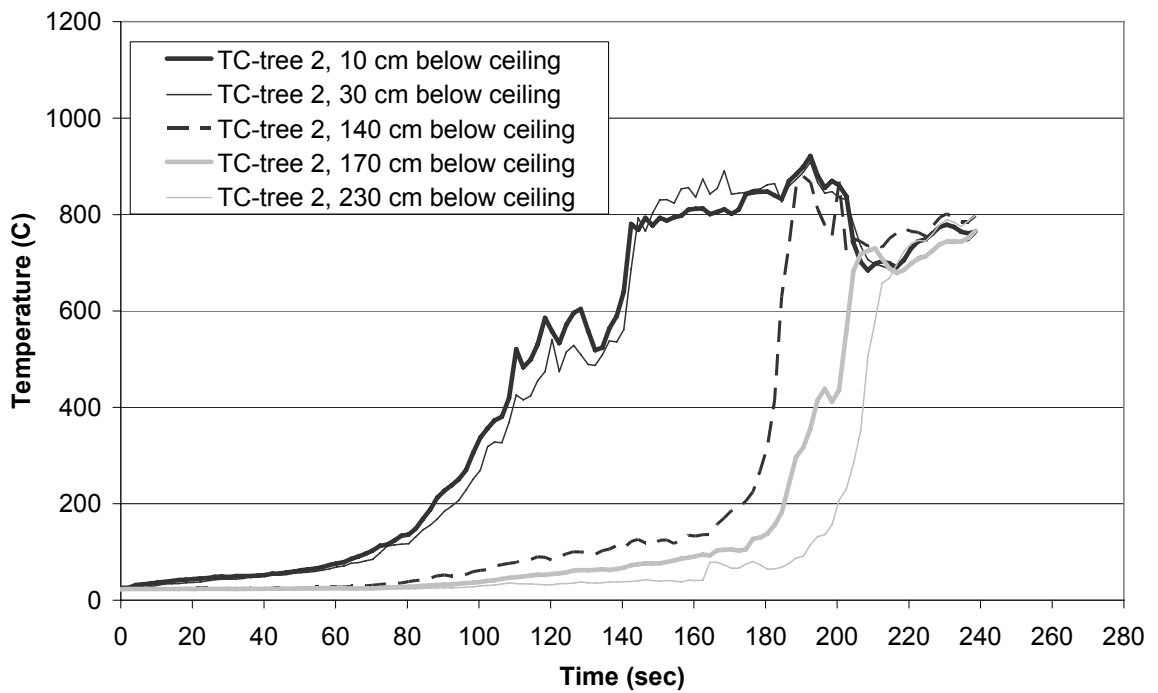


Figure 19 Measured temperatures in thermocouple tree 2. The positions of the thermocouple trees are shown in Figure 7.

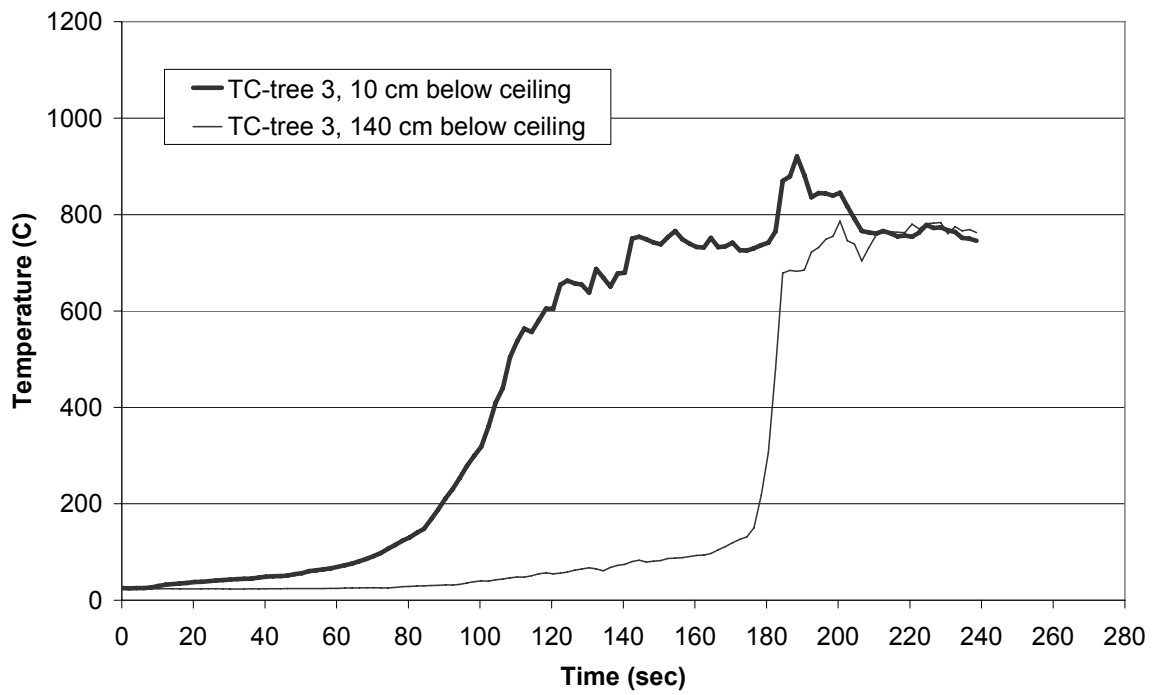


Figure 20 Measured temperatures in thermocouple tree 3. The positions of the thermocouple trees are shown in Figure 7.

The radiation measurement results are presented in Appendix A.

3 Material data

In this section the fire properties of materials used in the test are described. Important parameters include: heat release rate, ignition temperature, thermal conductivity, specific heat and heat of combustion.

3.1 Full scale tests of seat

The fire behaviour of the double seat was investigated twice, once free-burning in the furniture calorimeter and once burning inside the ISO 9705 room [12]. The reason why these two conditions were investigated was to see whether a slight change in ventilation would affect the fire dynamics. Figure 21 below shows the measurement equipment and the difference between the furniture calorimeter and the ISO 9705 room.

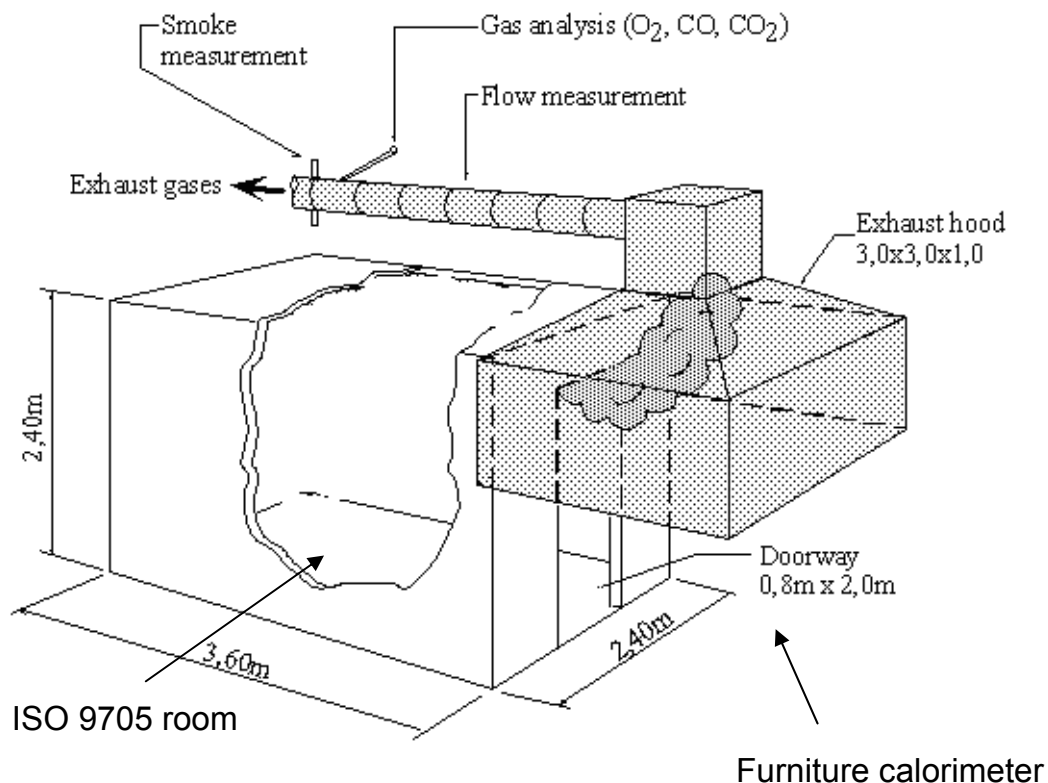


Figure 21 The ISO 9705 room test equipment. "Free-burning" in the furniture calorimeter means that the seat is placed directly under the exhaust hood. Burning inside the ISO 9705 room means that the seat was placed at the rear wall of the ISO 9705 room, see Figure 28.

3.1.1 Free-burning in the furniture calorimeter

Figure 22 to Figure 26 shows photos of the test in the furniture calorimeter. The results are shown in Figure 29.



Figure 22 Free-burning seat in the furniture calorimeter 36 s after ignition with the 7 kW propane burner.



Figure 23 Free-burning seat in the furniture calorimeter, 125 s after ignition.



Figure 24 Free-burning seat in the furniture calorimeter, 7 min and 39 s after ignition.

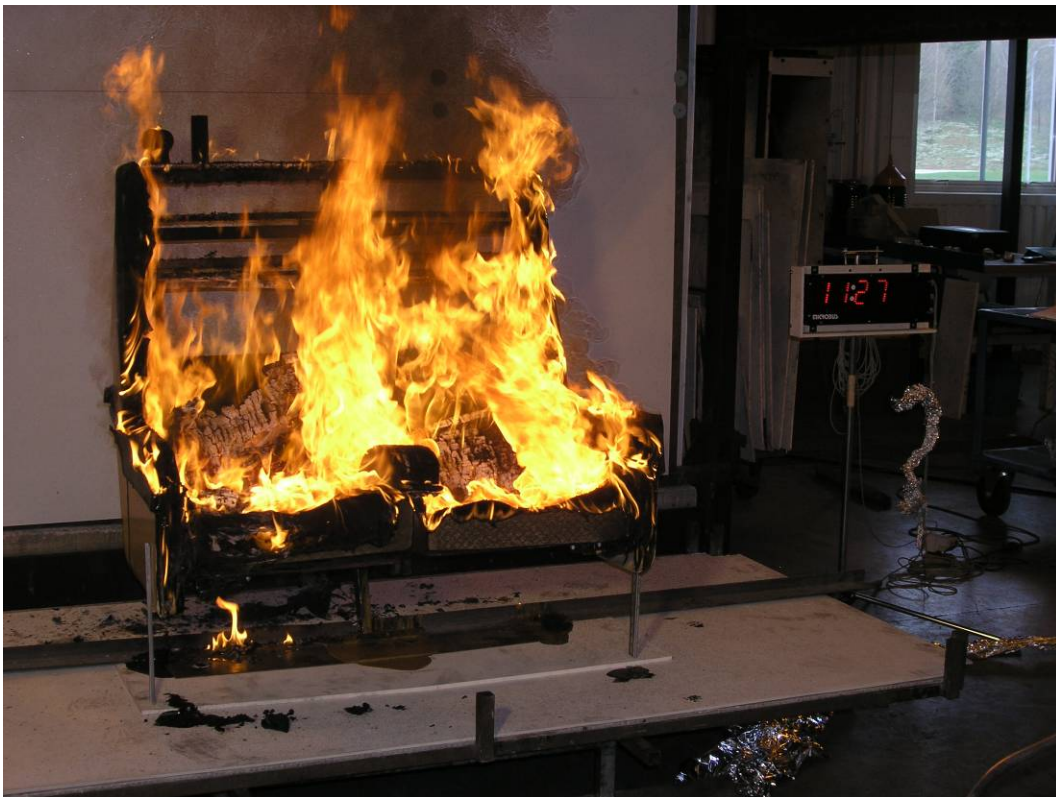


Figure 25 Free-burning seat in the furniture calorimeter, 11 min and 27 s after ignition.



Figure 26 Combusted seat after test in the furniture calorimeter.

3.1.2 Test in ISO 9705 room

Figure 27 and Figure 28 show photos of the test in the ISO 9705 room. The results are shown in Figure 29.



Figure 27 Seat tested in the ISO 9705 room. Ignition.



Figure 28 Burning seat in the ISO 9705 room, 6 min and 43 s after ignition.

3.1.3 Results

The heat release curves are shown in Figure 29. It can be seen that there is no significant difference in fire dynamics depending on whether the seat was free-burning in the furniture calorimeter or placed in the ISO 9705 room. However, it was seen that the fire of the ignited seat developed faster in the full scale test on the compartment. This can be explained by the fact that the compartment is much smaller than the ISO 9705 room and therefore a thicker and hotter smoke gas layer is developed. This is illustrated in Figure 49 where it is seen that Medtherm 64-2-18, which measures the radiation from the smoke gas layer in the full scale compartment test, yields a radiation level of 25 kW/m^2 . This radiation would by itself, without other ignition sources, ignite the seat within $\sim 30 \text{ s}$ as can be seen in Table 3.

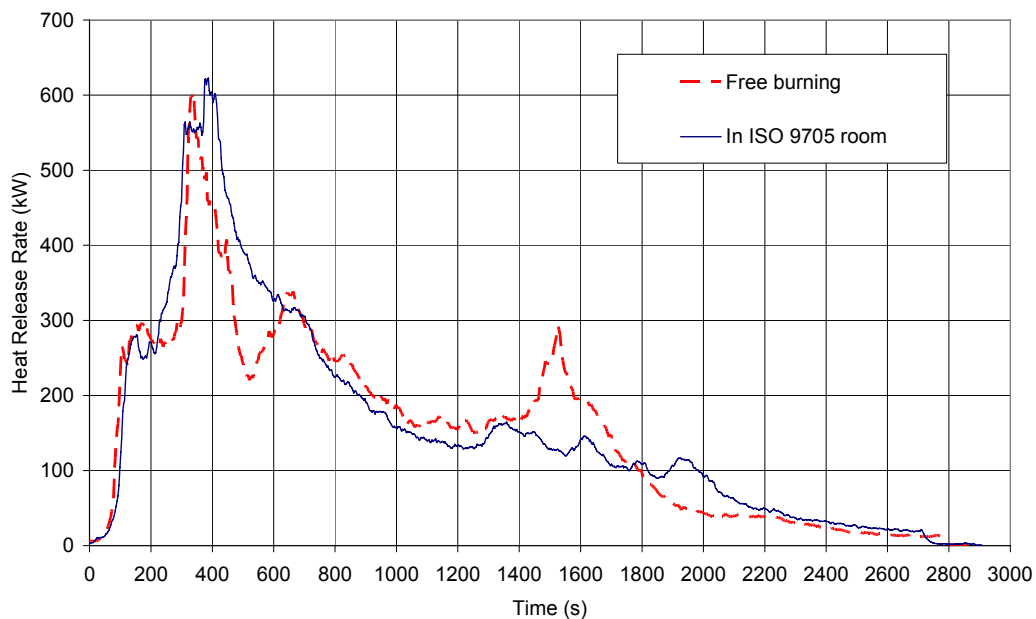


Figure 29 The heat release rates from the burning seats.

The total heat release was 441 MJ for the free burning seat and 454 MJ for the seat in the ISO 9705 room. The fire test with a free burning seat under the furniture calorimeter was performed with the seat positioned on a weight balance. The mass loss from the start of fire to extinction was 24.8 kg.

3.2 Small scale tests of seat, table, and lining materials

In this section results from the cone calorimeter are used to extract material parameters necessary for the FDS-simulations. Complete experimental results are presented in Appendix B.

3.2.1 Experimental setup

Materials were tested in the Cone Calorimeter, ISO 5660-1 [14], see Figure 30. Specimens of $0.1 \text{ m} \times 0.1 \text{ m}$ are exposed to controlled levels of radiant heating. The specimen surface is heated up and an external spark igniter ignites the pyrolysis gases

from the specimen. The time from start of irradiation to ignition of the sample is recorded and used in the analysis in Section 3.3.1 below.

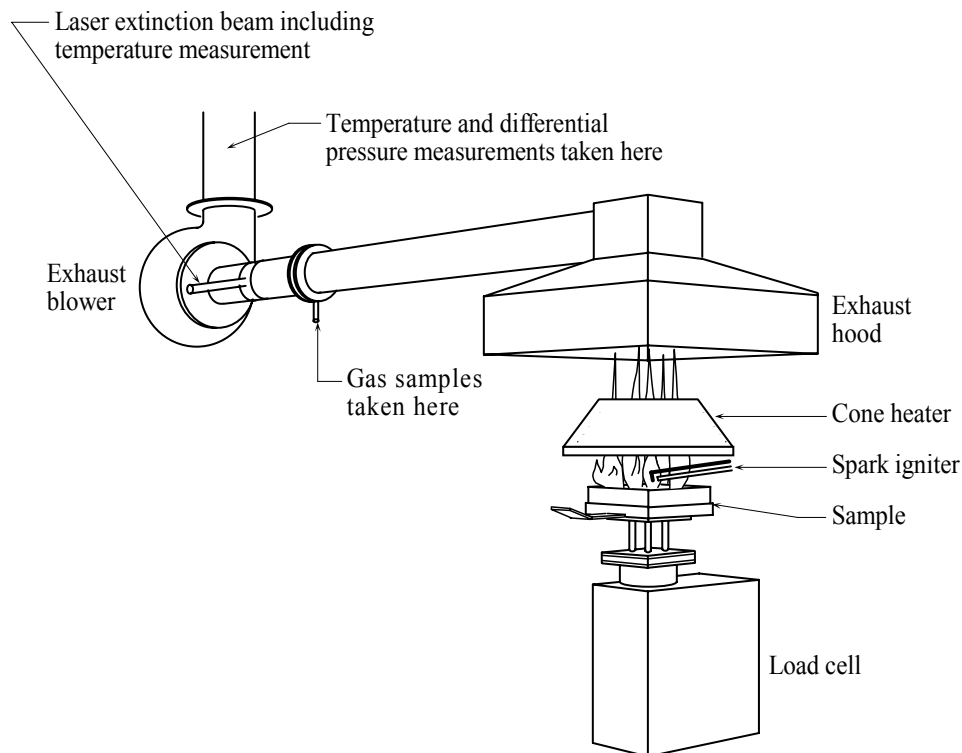


Figure 30 Schematic drawing of the Cone calorimeter, ISO 5660.

3.3 Ignition temperatures and thermal properties

A commonly used technique to evaluate temperature and thermal inertia is to measure the time it takes for a specimen to ignite in the cone calorimeter as a function of level of irradiation. A short summary of the theory is given below. More details on the background of the equations can be found in Babrauskas [15].

The method used here were suggested by Janssens [16, 17]. This method assumes that the materials are thermally thick, meaning that there is a 1-dimensional temperature gradient in the specimen. For the analysis of the results a system of three equations is solved. These equations are presented below without further explanations. The equations are:

Equation for heat flux equilibrium at critical heat flux:

$$\alpha_s \dot{q}_{cr} = h_c (T_{ign} - T_\infty) + \alpha_s \sigma (T_{ign}^4 - T_\infty^4) \quad \text{Equation 1}$$

The critical irradiation level \dot{q}_{cr} is defined as the point where a linear extrapolation of \dot{q} vs. $t_{ign}^{-0.55}$ crosses the x-axis, that is, the \dot{q} -axis, see Figure 31. It has been empirically found [15] that if the minimum irradiation level, \dot{q}_{min} , is substantially larger than \dot{q}_{cr} more realistic predictions of T_{ign} are obtained if \dot{q}_{cr} is replaced by \dot{q}_{min} . This was the case for metal laminate + plywood, seat, and PVC-carpet in the analysis below. \dot{q}_{min} is determined experimentally as the average of the lowest irradiation where ignition does occur and the highest irradiation where ignition does not occur.

Janssens' equation for thermally thick materials

$$q = q_{cr} \left[1 + 0.73 \left(\frac{K\rho C}{h_{eff}^2 t_{ign}} \right)^{0.55} \right] \quad \text{Equation 2}$$

Definition of effective convective coefficient:

$$h_{eff} = \frac{\alpha_s q_{cr}}{(T_{ign} - T_0)} \quad \text{Equation 3}$$

These equations are solved for T_{ign} and $K\rho C$ numerically, using Kelvin and not °C as the unit for temperature. The results are presented in Section 3.3.1 below.

3.3.1 Results and analysis

The experimental results are summarized in Table 3 below and the graphs with q vs. $t_{ign}^{-0.55}$ are shown in Figure 31 to Figure 35.

Table 3 Time to ignition, t_{ign} , as a function of irradiation level for the materials tested in the cone calorimeter.

Irradiation, \dot{q} [kWm ⁻²]	Time to ignition, t_{ign} [s]				
	Seat	Metal laminate	HPL Laminate	PVC-carpet	Table
7.5	*	*	*	**	*
10	**	**	**	168	**
15	82	**	**	110	**
25	31	**	**	38	162
35	14	**	575	26	101
50	11	77	110	12	38
75	3	46	14	7	22

* No test

** No ignition

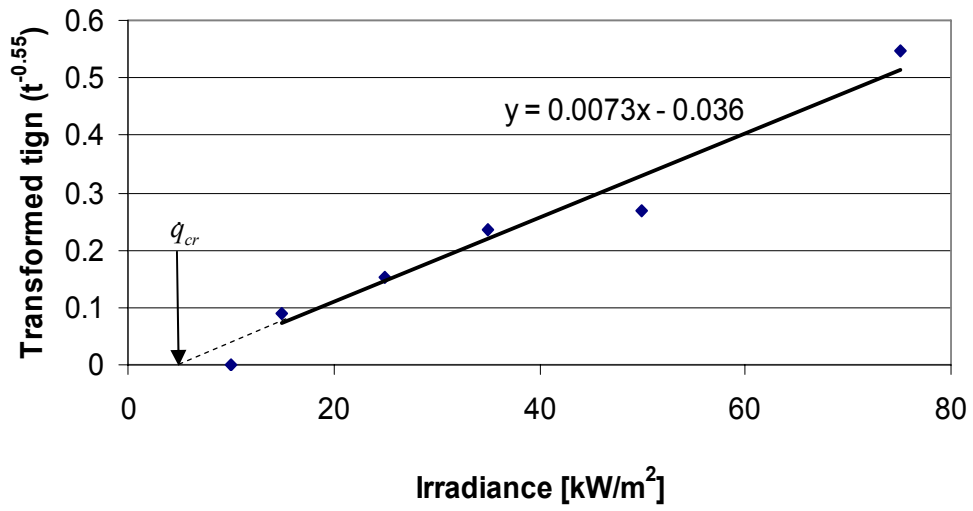


Figure 31 Seat.

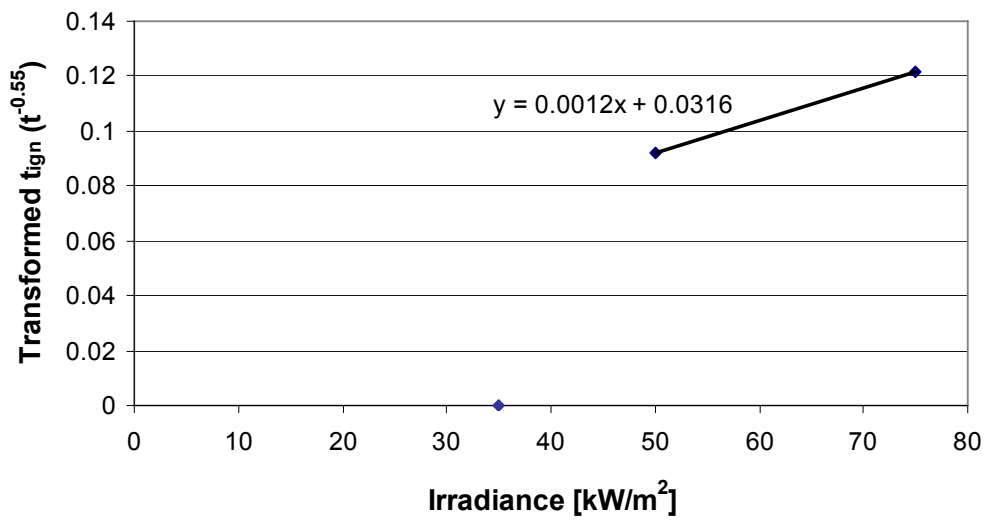


Figure 32 Metal laminate on plywood.

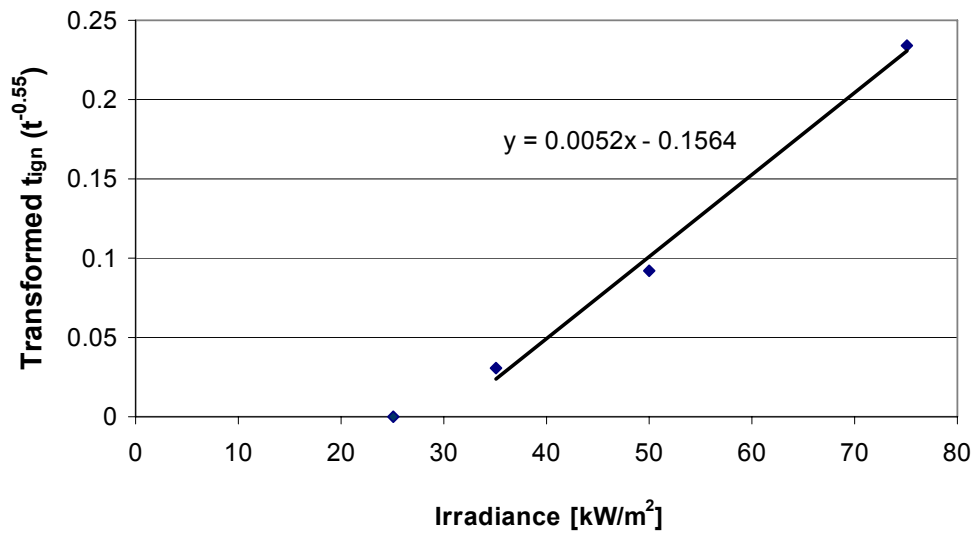


Figure 33 HPL-laminate on plywood.

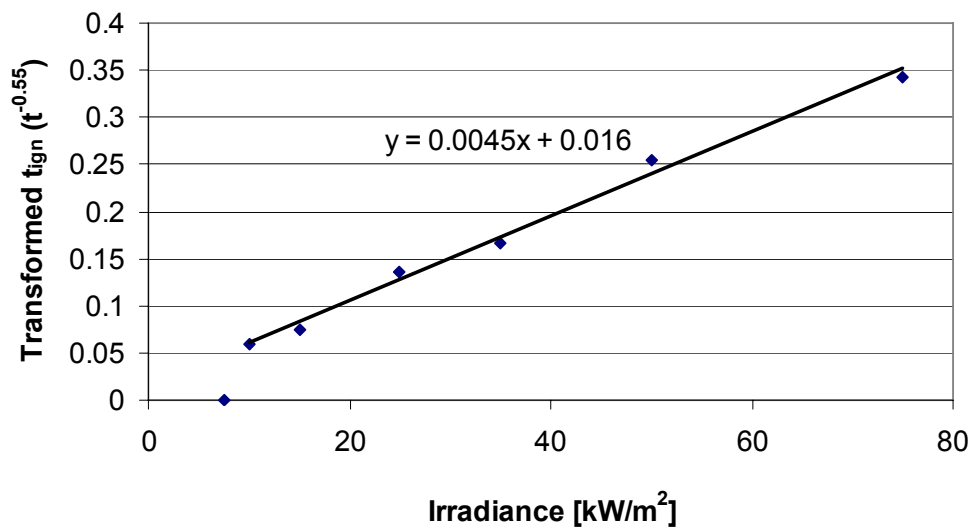


Figure 34 PVC carpet.

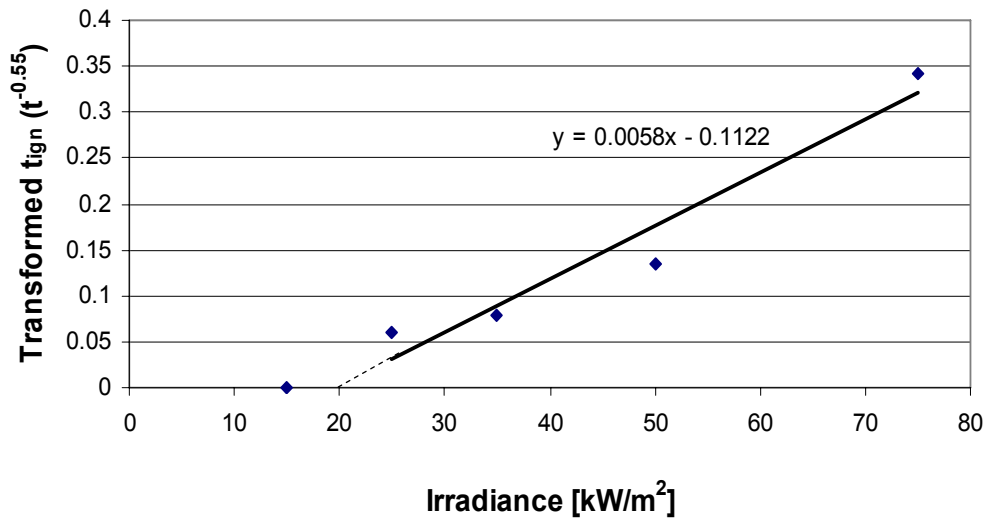


Figure 35 Wood table

The surface absorptivity is set to 0.9 and the convective coefficient to $0.013 \text{ kWm}^{-2}\text{K}^{-1}$ when Equation 1 to Equation 3 are solved for T_{ign} and $K\rho C$. The results are given in Table 4 below.

Table 4 Ignition temperatures and thermal inertias obtained from the experiments.

	Seat	Metal laminate	HPL-laminate	PVC-carpet	Table
Ignition temperature, T_{ign} [°C]	346	607	526	278	433
Thermal inertia, $K\rho C$ [$\text{J}^2\text{m}^{-4}\text{s}^{-1}\text{K}^{-2}$]	$1.68 \cdot 10^5$	$1.74 \cdot 10^6$	$1.51 \cdot 10^5$	$6.11 \cdot 10^5$	$1.73 \cdot 10^5$

In order to simulate the fire using FDS it is not enough to know the thermal inertia $K\rho C$ but specific information is needed for the thermal conductivity K , the density ρ , and the specific heat C .

Seat

The seat consists of fabric on PUR foam upholstery. Separate values for K , ρ , and C will be obtained by selecting a value for C from the literature, calculate ρ from the measured weight and volume data, and thereafter extract K from the thermal inertia. It might be questioned if a material such as fabric + PUR-foam can be investigated with the Janssens' method. Since melting occurs some of the energy will be channelled to a phase change instead of to increasing the temperature. On the other hand, if the melting occurs rapidly the studied material will in fact not be a foam but rather a molten, higher density, foam. Given the value of $K\rho C$ obtained in this study it is possible to obtain consistent results with realistic separate values for K , ρ , and C only if a PUR in molten foam is assumed.

The specific heat for PUR is $\sim 1400 \text{ JK}^{-1}\text{kg}^{-1}$ [18] and that of the fabric (polyethylene terephthalate, PET, or polyester) is $1000 \text{ JK}^{-1}\text{kg}^{-1}$ [19]. Therefore a value of $1200 \text{ JK}^{-1}\text{kg}^{-1}$ has been chosen.

The measured density of the seat was measured to 77 kgm^{-3} .

Deriving K from $K\rho C$, ρ , and C gives the thermal parameters:

Thermal conductivity K :	$1.8 \text{ Wm}^{-1}\text{K}^{-1}$
Density ρ :	77 kgm^{-3}
Specific heat C :	$1200 \text{ JK}^{-1}\text{kg}^{-1}$

Whether the PUR should be considered as foam or liquid/solid is further discussed in Section 6.1.2.

Metal laminate

The material consists of 1.6 mm metal laminate glued onto 18 mm plywood. The strategy for obtaining separate values for K , ρ , and C will also here be to select a value for C from the literature, calculate ρ from the measured weight and volume data, and thereafter extract K from the thermal inertia.

The specific heat for aluminium is $896 \text{ JK}^{-1}\text{kg}^{-1}$ [20] while typical values for wood are around $2500 \text{ JK}^{-1}\text{kg}^{-1}$ [20]. Since the thermal conductivity of aluminium is very high and since the major part of the material is plywood the specific heat of this material is simply set to $2500 \text{ JK}^{-1}\text{kg}^{-1}$. The measured density of the composite metal laminate + plywood material was measured to 648 kgm^{-3} . This results in a value of $1.07 \text{ Wm}^{-1}\text{K}^{-1}$ for the thermal conductivity of the composite material. The thermal conductivity for the metal is $204 \text{ Wm}^{-1}\text{K}^{-1}$ and on the order of $0.1 \text{ Wm}^{-1}\text{K}^{-1}$ for wood [20].

Summing up, the thermal parameters that is used in the modelling are:

Thermal conductivity K :	$1.07 \text{ Wm}^{-1}\text{K}^{-1}$
Density ρ :	648 kgm^{-3}
Specific heat C :	$2500 \text{ JK}^{-1}\text{kg}^{-1}$

HPL-laminate (High Pressure Laminate)

The material consists of 1 mm HPL laminate glued onto 18 mm plywood. The strategy for obtaining separate values for K , ρ , and C will be the same as for the metal laminate + plywood composite, that is, to select a value for C from the literature, calculate ρ from the measured weight and volume data, and thereafter extract K from the thermal inertia.

The specific heat is on the order of $1.4 \cdot 10^3 \text{ JK}^{-1}\text{kg}^{-1}$ for paper and for phenol [21, 22]. No value has been found for the specific heat of melamine resin. Given the small amount of HPL-laminate compared to the amount of plywood the value used for the HPL laminate + plywood is the same as the typical specific heat for wood, $2500 \text{ JK}^{-1}\text{kg}^{-1}$. The density of the material was measured to 548 kgm^{-3} . This results in a value of $0.11 \text{ Wm}^{-1}\text{K}^{-1}$ for the thermal conductivity of the composite material.

Summing up, the thermal parameters that is used for the HPL laminate in the modelling are:

Thermal conductivity K :	$0.11 \text{ Wm}^{-1}\text{K}^{-1}$
Density ρ :	548 kgm^{-3}
Specific heat C :	$2500 \text{ JK}^{-1}\text{kg}^{-1}$

PVC carpet

Properties for PVC can be obtained from Goodfellow [23]:

Thermal conductivity K :	0.12-0.25 $\text{Wm}^{-1}\text{K}^{-1}$ (at 23°C)
Density ρ :	1400 kgm^{-3}
Specific heat C :	1000-1500 $\text{JK}^{-1}\text{kg}^{-1}$

These values are for unplasticised PVC while PVC carpets typically have some degree of plasticiser, as well as pigmentation. It is assumed that this has no significant importance for the fire properties of the PVC carpet. Multiplying K , ρ , and C gives a thermal inertia on the lower side of the experimentally obtained value $6.11 \cdot 10^5 \text{J}^2\text{m}^{-4}\text{s}^{-1}\text{K}^{-2}$. Therefore the high end values are used for conductivity and specific heat.

The thermal parameters that are used for the PVC carpet in the modelling are:

Thermal conductivity K :	0.25 $\text{Wm}^{-1}\text{K}^{-1}$
Density ρ :	1400 kgm^{-3}
Specific heat C :	1500 $\text{JK}^{-1}\text{kg}^{-1}$

This gives a thermal inertia $K\rho C$ of $5.25 \cdot 10^5 \text{J}^2\text{m}^{-4}\text{s}^{-1}\text{K}^{-2}$ which is in fair agreement with experiment.

Wood table

The wood table was 30 mm thick and consisted of plywood with a thin, ~1 mm, HPL laminate layer on top. The laminate material was similar to the tested HPL laminate. The strategy for obtaining separate values for K , ρ , and C will be the same as for the metal laminate and the HPL laminate, that is, to select a value for C from the literature, calculate ρ from the measured weight and volume data, and thereafter extract K from the thermal inertia. Given the small amount of HPL laminate compared to the amount of plywood the value used for the HPL laminate + plywood is the same as the typical specific heat for wood, $2500 \text{JK}^{-1}\text{kg}^{-1}$. The density of the wood table was measured to 616kgm^{-3} . This results in a value of $0.11 \text{Wm}^{-1}\text{K}^{-1}$ for the thermal conductivity of the composite material.

Summing up, the thermal parameters that is used for the wood table in the modelling are:

Thermal conductivity K :	0.11 $\text{Wm}^{-1}\text{K}^{-1}$
Density ρ :	616 kgm^{-3}
Specific heat C :	2500 $\text{JK}^{-1}\text{kg}^{-1}$

4 Standardized design fires – Pre-flashover t^2 fires

The International Standardization Organisation, ISO, recommends the following equation for pre-flashover design fires [24]:

$$\dot{Q} = \dot{Q}_0 \left(\frac{t}{t_g} \right)^2$$

Equation 4

Where \dot{Q}_0 is 1 MW and t_g defines the time scale of the fire growth according to Table 5 below.

Table 5 Characteristic time scales for the different growth rates for pre-flashover design fires [24].

Growth rate description	Characteristic time, t_g (s)
Slow	600
Medium	300
Fast	150
Ultra fast	75

The design fires prescribed according to Equation 4 are shown in Figure 36 together with the experimental result from the full scale experiment. It can be seen that two of the curves reproduce the experimental results to a reasonable degree. The “Fast” design fire with $t_g=150$ s manages to reproduce the time to flashover (~ 180 s) fairly well. The post-flashover heat release is, however, underestimated. On the other hand the pre-flashover t^2 fires are, as the name suggests, not meant to give information concerning the dynamics of vitiated post-flashover fires. One way of getting a better reproduction of the experimental results is to use the “Ultra fast” design fire with $t_g=75$ s and shift it in such a way that it starts when the heat release rate has reached a threshold of 50 kW. In this way the post-flashover heat release rate is better reproduced, although far from perfectly. It should be noted that this design fire, the shifted “Ultra fast” fire, also manages to reproduce time to flashover fairly well. The threshold value of 50 kW is not arbitrary but corresponds approximately to a wastebasket and is a HRR that with high probability will be detected [25]. The rationale for such a threshold is that for very small fires the sensitivity to the actual original fire source (seats of different materials, non-vandalized seats or seats vandalized to different degrees, wastebasket, etc.) becomes very large. In other words, once the original fire source has started to release heat the initial dynamics can be very different. The initial dynamics will, for example, be very different whether a seat is ignited with a cigarette, with a 7 kW prCEN/TS 45545 burner [13], or with a 30 kW CBUF burner [25]. If a cigarette is used to ignite a seat (the seat is the original fire source), a smouldering fire could start and the time before the entire seat burns would be highly unpredictable. Using a threshold corresponding to heat source as powerful as a wastebasket ensures that the original fire source has a significant impact on the entire compartment once the t^2 curve is implemented.

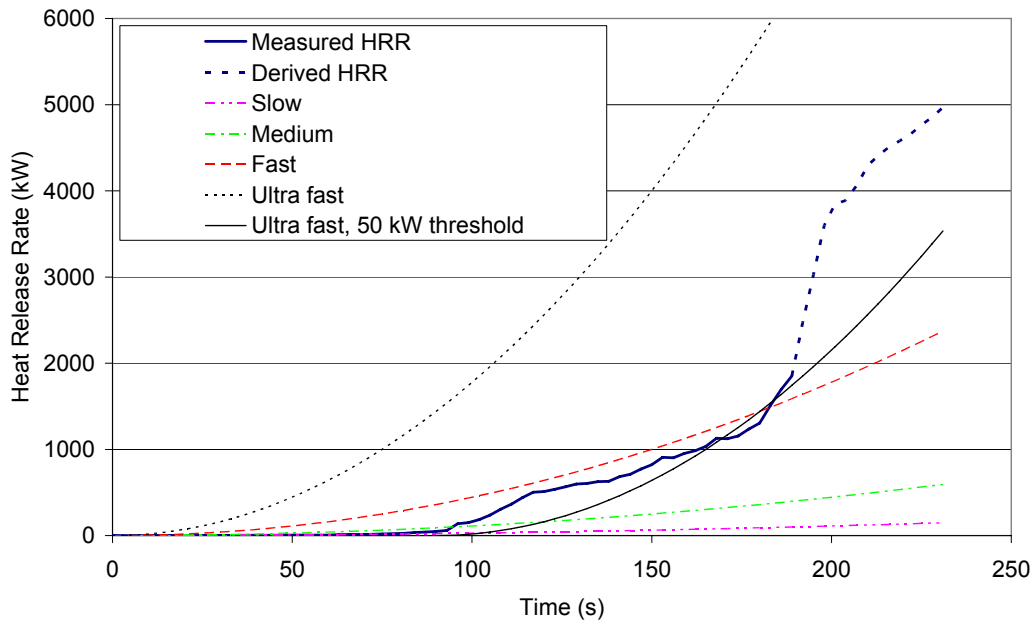


Figure 36 Design fires with different characteristic time scales according to reference [24]. The experimental results from Figure 12 are also included. "50 kW threshold" means that the curve has been shifted along the time-axis in such a way that it begins when experimentally measured heat release reaches 50 kW. This occurs at $t=90$ s.

5 Design fires by analytical methods – Superpositioning of HRR curves

One method to construct a design fire is to basically add up the contributions of HRR from the burning objects in the compartment. This method is only applicable for fuel controlled fires, or pre-flashover fires, for which the access to oxygen is not a limiting factor. This method has three major limitations when used to calculate a design fire: 1) access to oxygen is not taken into consideration, 2) without running a full scale test it is not known at what time each object will ignite and 3) the extra increase in HRR from each object due to irradiation from the other burning objects is not included in the total HRR.

5.1 Example 1

To see how close it is possible to get to the “right answer”, in this case the experimental curve, when only taking the seats into consideration, the ignition times observed in the test were used. The result is presented in Figure 37. The grey solid and dotted lines represent the HRR from the test of the full train compartment. The thin black line is the HRR of the single seat burning in the ISO 9705 room, presented in 3.1.2. The black dotted line is the same curve with the incipient phase cut out. The incipient phase is taken as the time before the HRR curve takes off after reaching 60 kW. The curve is representative for only one burning seat, i.e., it is cut off before the second seat in the double-seat arrangement ignites. The black thick line is the sum of the HRR from 6 burning seats where the HRR curve for each seat is delayed in time depending on when it ignites in the full scale test. The first seat is ignited by the same burner used in the compartment test, thus the incipient phase is included. According to the observations from the full scale test the two following seats ignited at 140 and 150 s respectively, and the 3 seats in the left row ignited simultaneously at 180 s. The superposition of the curves was done using a simple excel spread sheet.

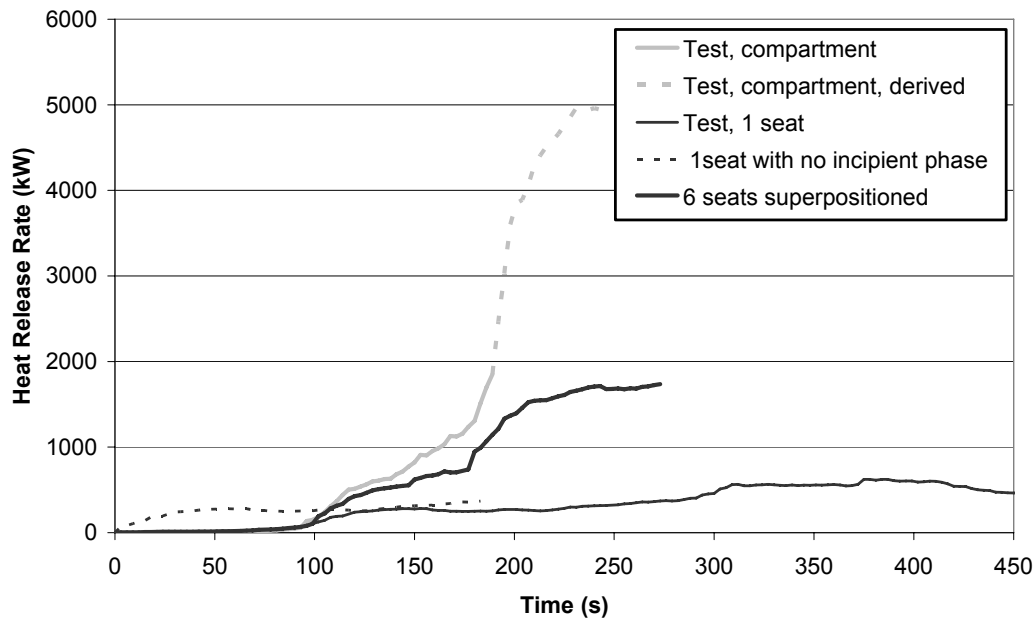


Figure 37 Example 1 - Superposition of the HRR of 6 free burning seats that ignite at the times observed in the full scale compartment test.

5.2 Example 2

Using superposition of HRR curves, the shorter the ignition times used for each product in the room, the more the resulting HRR curve will represent a worst case scenario. With no knowledge about the sequence of ignitions of seats one could assume the worst case would be that all seats ignite simultaneously, together with the first seat. The black line in Figure 38 shows the curve obtained if six HRR curves of one free burning seat (including the incipient phase) are superimposed with no time delay between the ignitions. The noticeable increase in HRR up to 100 s is the effect of the fact that the HRR measured during the incipient phase is multiplied by 6. In reality the HRR is zero from the other five seats while the incipient phase of the first seat is going on.

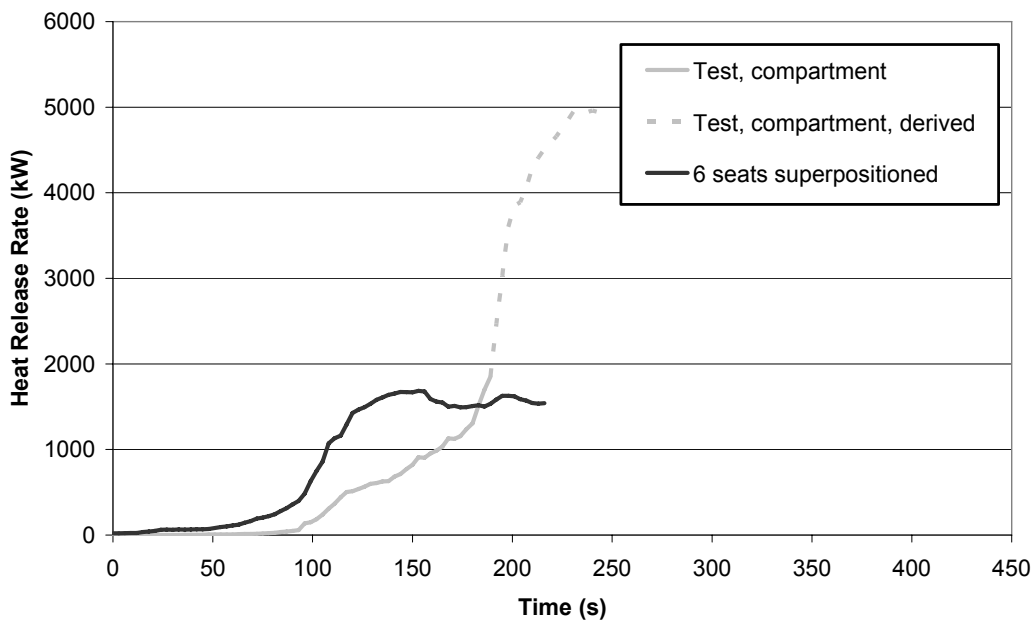


Figure 38 Example 2 - Superposition of the HRR of 6 free burning seats that ignites by a burner at time zero (black line),

The HRR curve reaches the level of flashover approximately 1 minute prior to when it actually occurred in the real test. The HRR after flashover is greatly underestimated.

5.3 Example 3

In the previous example it was assumed the seats had the major impact on the fire dynamics. In this example the other materials in the compartment will also be included in the HRR calculation. The black line in Figure 1 shows the result if an estimate of the contribution from the other combustible products and lining materials in the room is also included. The contribution in HRR from the walls (upper half of the room), the table and the luggage rack was calculated by multiplying the HRR from the 50 kW/m² cone calorimeter tests by the exposed area of each product, i.e. it is assumed that all seats ignite and burn as the free-burning seats and that all other surfaces in the room are subjected to a heat flux of 50 kW/m² from the moment of ignition.

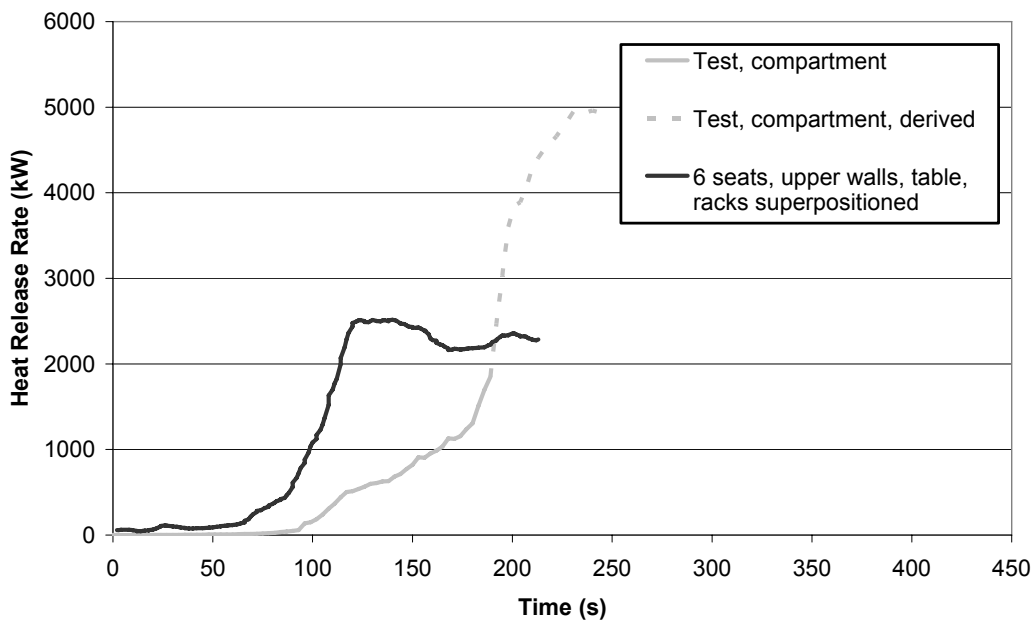


Figure 39 Example 3 - Superposition of the HRR of 6 free-burning seats that are ignited by a burner at time zero and HRR from other products in the room calculated as the HRR obtained in cone calorimeter tests multiplied by each products exposed surface area.

The floor is excluded in the calculation since ignition is known to normally occur at times around flashover. Including the floor in the calculation from time zero would have an unrealistic impact on the increase of the HRR at the pre flashover phase. However, to obtain a better estimate of the HRR at post-flashover, the contribution of HRR from the floor should be included, beginning at a time around flashover. In this case the maximum of the total HRR curve would be approximately 1 MW higher if the floor were included in the model (not shown in the graph).

6 Design fires by CFD field modelling – FDS5

A more sophisticated method to calculate the HRR curve of the burning train compartment, using Computational Fluid Dynamics (CFD), is described below. The field model used here is the Fire Dynamics Simulator, FDS, version 5, developed by the National Institute of Standards and Technology, NIST. FDS was developed with an emphasis on flows typically occurring during a fire, i.e., low-speed and thermally-driven flows, and models turbulence using the Large Eddy Simulation (LES) technique [26]. The program includes several sub-models for modelling phenomena associated with fire such as combustion, radiation, heat transfer, and pyrolysis.

In our model the fire growth and the resulting HRR curve will be calculated by simulating the flame spread in the compartment originating from the fire in the burner on the seat. The flame spread is modelled by heat transfer through convection and radiation. As a surface reaches a user specified ignition temperature, that part of the surface ignites and burns following a pre-defined HRR curve. As was the case for the real test, the walls, floor and furniture are combustible in the model, the window and ceiling are non-combustible.

6.1 Model

6.1.1 Geometry

The geometry of the FDS model is the same as for the tested compartment. The model includes a $1.4 \text{ m} \times 2.0 \text{ m} \times 3.5 \text{ m}$ high space outside the door to make sure that all the fuel vaporized in the compartment is combusted within the simulation domain even after flashover is reached. This is to include the combustion in the calculation of the HRR. The geometry is shown in Figure 40. The black rectangle on the seat to the left in the figure, is the burner. The green dots mark the location of the thermocouples. The mesh consisted of 224 000 cells with the size $50 \text{ mm} \times 50 \text{ mm} \times 50 \text{ mm}$.

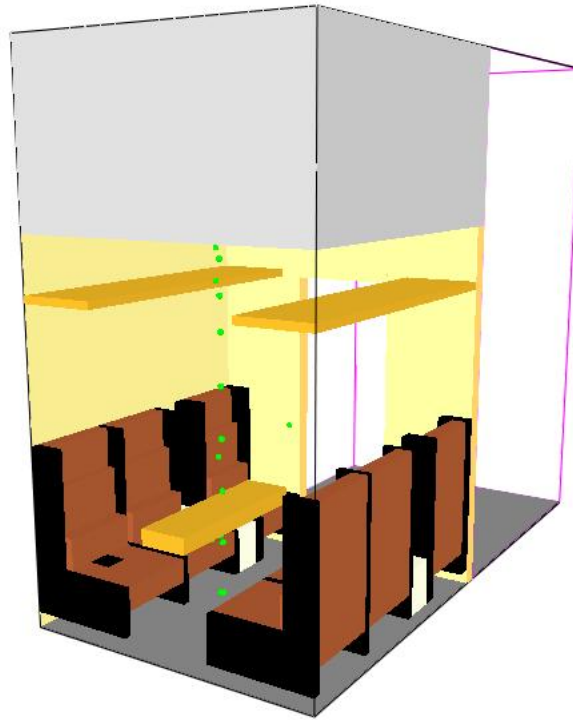


Figure 40 Geometry of FDS model. Two walls are transparent in the figure for visualization purposes.

6.1.2 Material properties

For each material in the model the thickness, thermal conductivity ($\text{Wm}^{-1}\text{K}^{-1}$), specific heat ($\text{JK}^{-1}\text{kg}^{-1}$), density (kgm^{-3}) and thickness (m), is specified. If the material is combustible, the ignition temperature ($^{\circ}\text{C}$), heat of combustion (kJkg^{-1}) and a curve for the heat release rate (kWm^{-2}) vs. time (s) is added to the list of input parameters. The material properties for the walls, floor and table, and to some extent the seat, were determined from the cone calorimeter tests. The values were either directly measured in the test method or calculated based on the test results. The methods used and the extracted material parameters are described in Section 3.3. Since the material in the luggage rack were not tested in the cone calorimeter and the major part consisted of wood the material properties for the wood table were used.

The heat release curves for each material in the model are the curves obtained in the cone calorimeter tests. Which curve that is most appropriate to use, i.e., the 35, 50 or 75 kW/m^2 curve, must be considered with care. Since the curve dictates the rate by which the surface burns the curve must correspond to the irradiation the surface is exposed to from the room but also from its own flames. Furthermore, in a cone calorimeter test the specified heat flux levels is the incident flux from the cone to the radiometer before the test. When the surface is burning there is a contribution of irradiation from the flames. In the EUREFIC program the heat exposure to a ceiling in a room corner test when the flame front just had passed were measured to 50 kW/m^2 [27]. This is also the irradiation level that has been used successfully in the simulation program Conetools (the SBI model) described in Section 7.2. Therefore, for most materials, the cone calorimeter curve obtained at the irradiation level of 50 kW/m^2 was used. In the

project CBUF [25] the incident flux to burning seat cushions was measured. Based on the results of the tests, the data from the 35 kW/m^2 cone calorimeter tests were used in the following discussions and predictions of burning rate in the CBUF project. It was therefore decided in this project to follow the recommendations of CBUF for the seats and the heat release rate curve obtained at 35 kW/m^2 were used.

The seats were modelled using the same material properties over the whole surface. The properties were based on the 5 cm thick sample of foam covered by lining fabric, tested in the cone calorimeter. The heat release curve specified in the model is kept constant from 5 minutes and forward since the second peak around 8 minutes (see Appendix B, Figure 1) may be a boundary effect of the melting PUR foam and not representative for other foam thicknesses. The thermal conductivity determined in Section 3.3.1 is questionable, see discussions in the same chapter. The value of $1.8 \text{ Wm}^{-1}\text{K}^{-1}$ is unrealistically high for a flexible PUR foam. It may be suitable for melted PUR but since the seat cushion consists of unmelted foam during most of the simulation time it comes to no surprise that this value had to be decreased to obtain proper temperature rise and finally ignition of the surface. The parameter was adjusted until adequate agreement for the HRR increase up to flashover between the simulation results and the test results was achieved. A value of $0.015 \text{ Wm}^{-1}\text{K}^{-1}$ was found to give acceptable correlation, which is reasonable for a PUR foam.

The reaction in the gas phase was specified to be combustion of PUR. All other FDS-are kept as their default values.

6.2 Results

A visualisation of the flame and smoke development in the FDS model is presented in Figure 41. The views and the times are similar to when photos from the test, presented in Section 2.2.3, were taken.

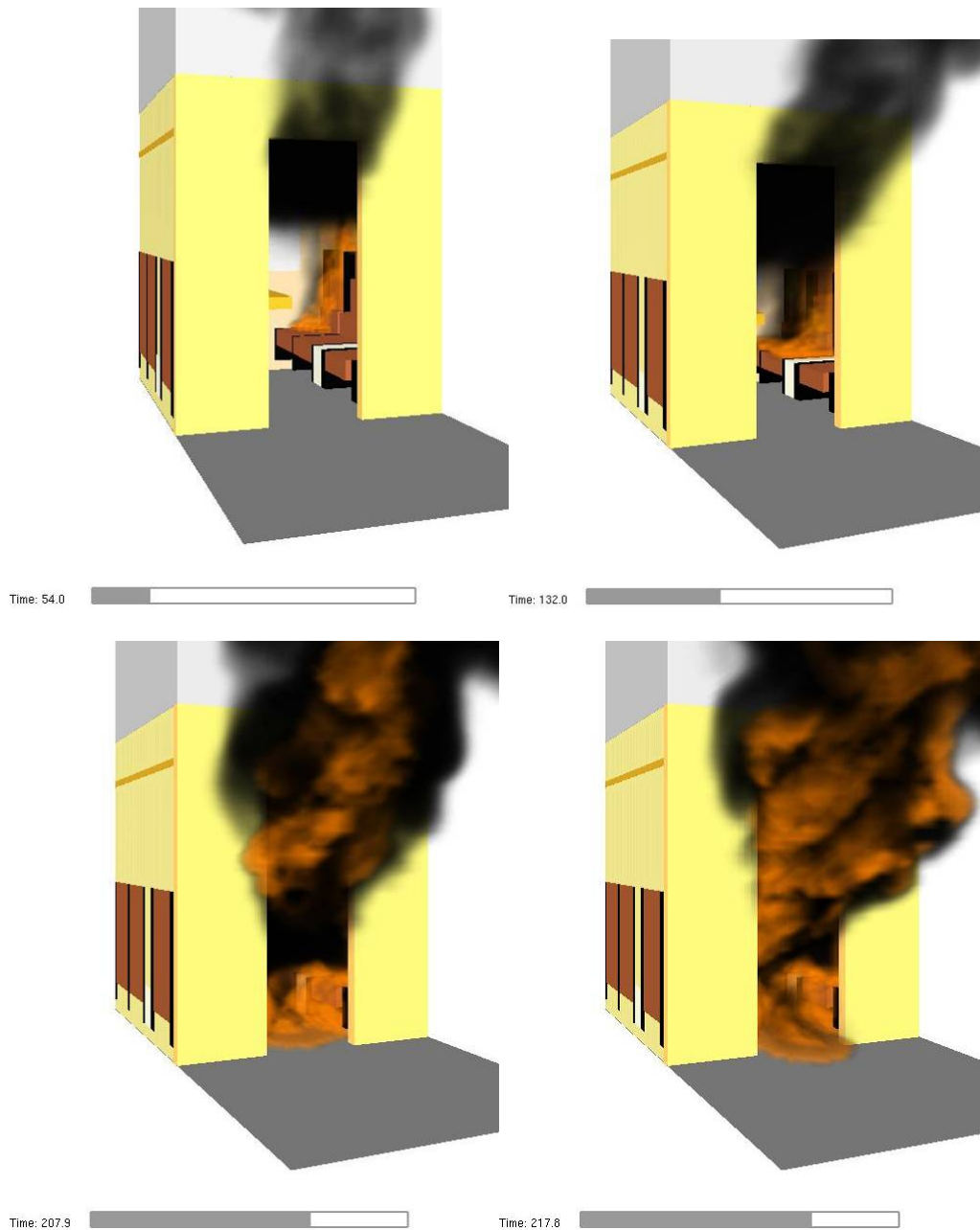


Figure 41 Flame and smoke development in FDS model at 54, 132, 208 and 218 s after ignition.

The HRR and gas temperature are plotted in Figure 42 to Figure 47. Flame spread and the sequence of items being ignited is initially faster in the FDS model compared to the test, which explains the higher HRR for the period up to 100 s after ignition. This causes higher gas temperatures close to the ceiling in the model up to approximately 80 s. From approximately 100 s to 180 s there is an increase in HRR in the test which is delayed in the FDS model and causes a faster increase of the temperatures in the gas top layer in the test as compared to the model. The gas temperatures at the mid-height and floor level follow the temperatures from the test relatively well until after flashover when the TCs in the model are surrounded by flames and show temperatures above 1000 °C.

It should be noted that the FDS simulation is not a prediction, the test result was known at the time of the simulation. The thermal conductivity of the material in the seats was tuned until satisfactory correlation with the test results in HRR was achieved. All other parameters were kept at the values determined in section 3.3.1.

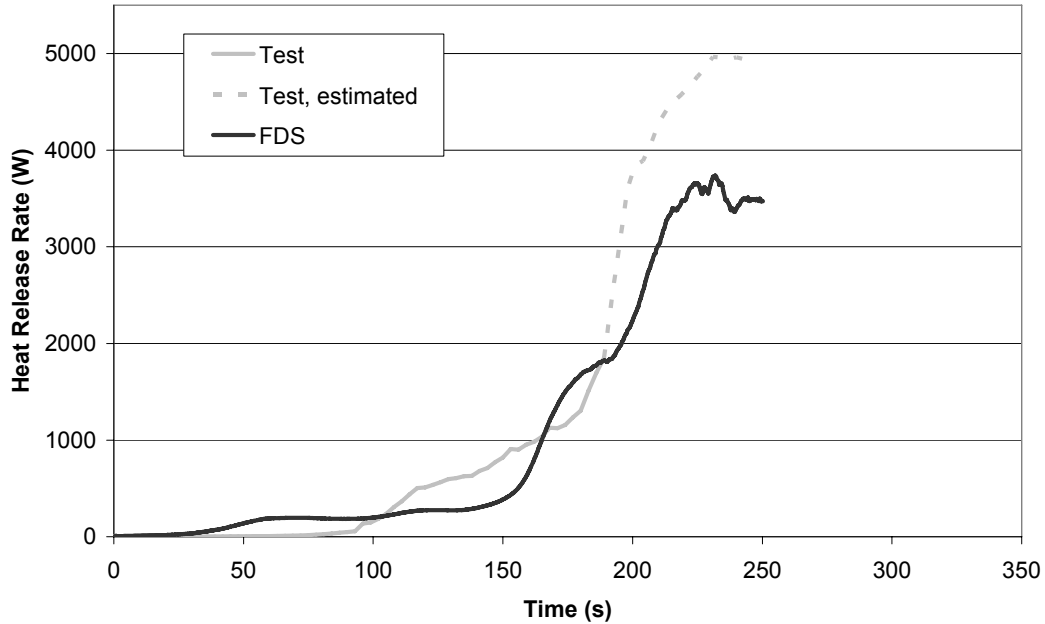


Figure 42 Experimental HRR results from the full scale test in gray. The simulated result is shown in black.

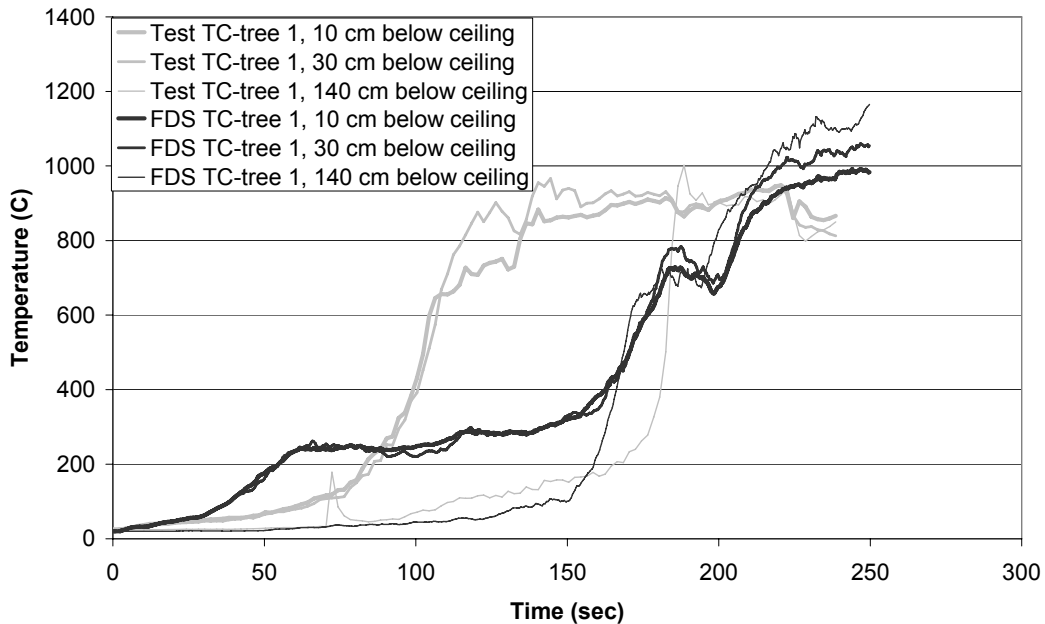


Figure 43 Experimental (grey) and FDS (black) results for temperatures measured by TC-tree 1 (see Figure 4) 10 – 140 cm below the ceiling.

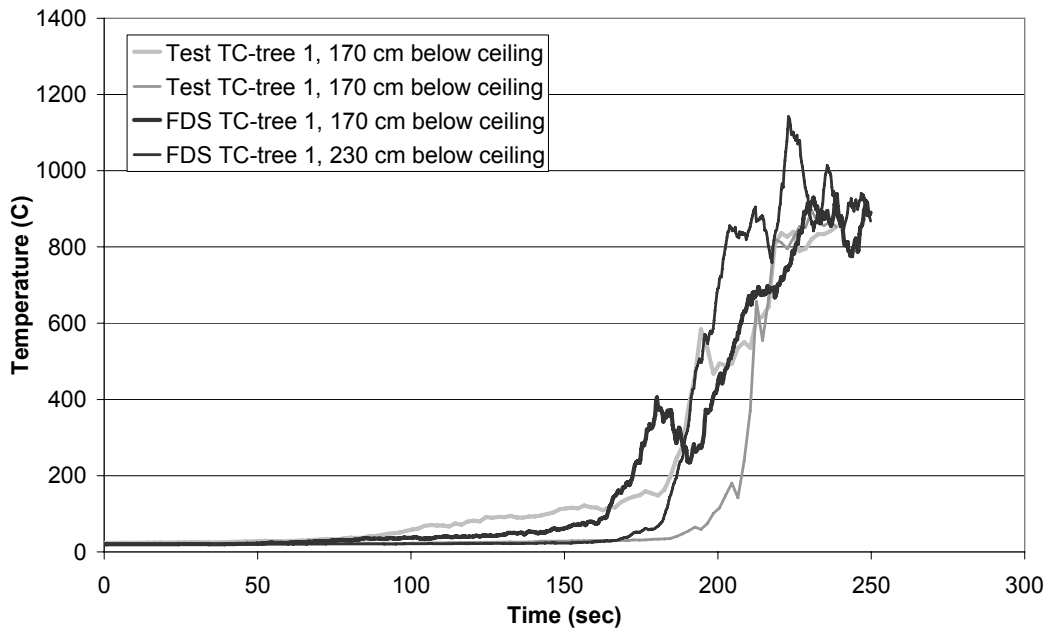


Figure 44 Experimental (grey) and FDS (black) results for temperatures measured by TC-tree 1 (see Figure 4) 170 – 230 cm below the ceiling.

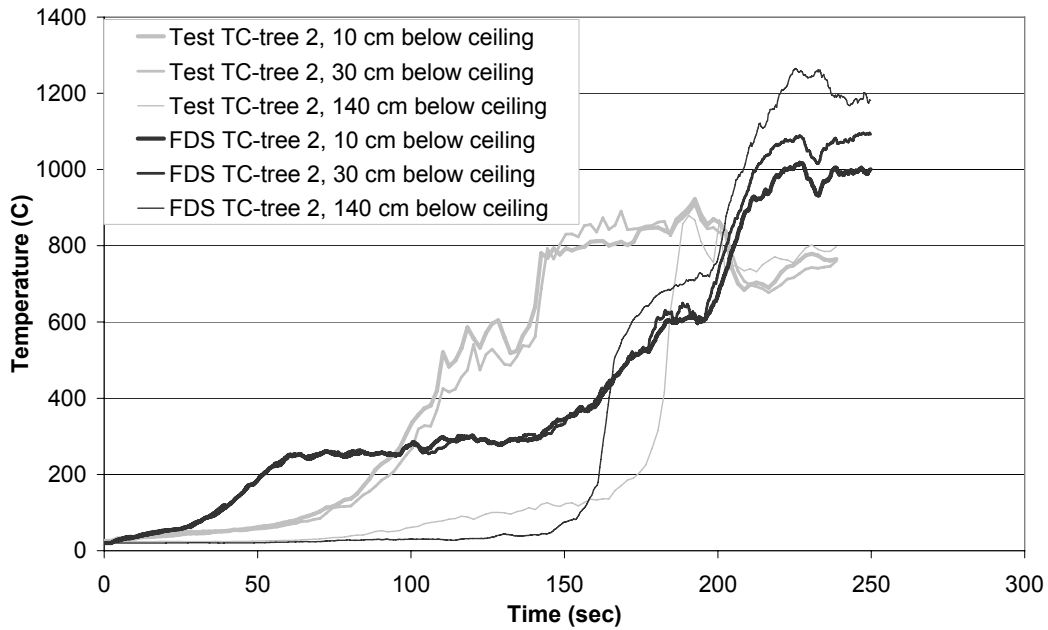


Figure 45 Experimental (grey) and FDS (black) results for temperatures measured by TC-tree 2 (see Figure 4) 10 – 140 cm below the ceiling.

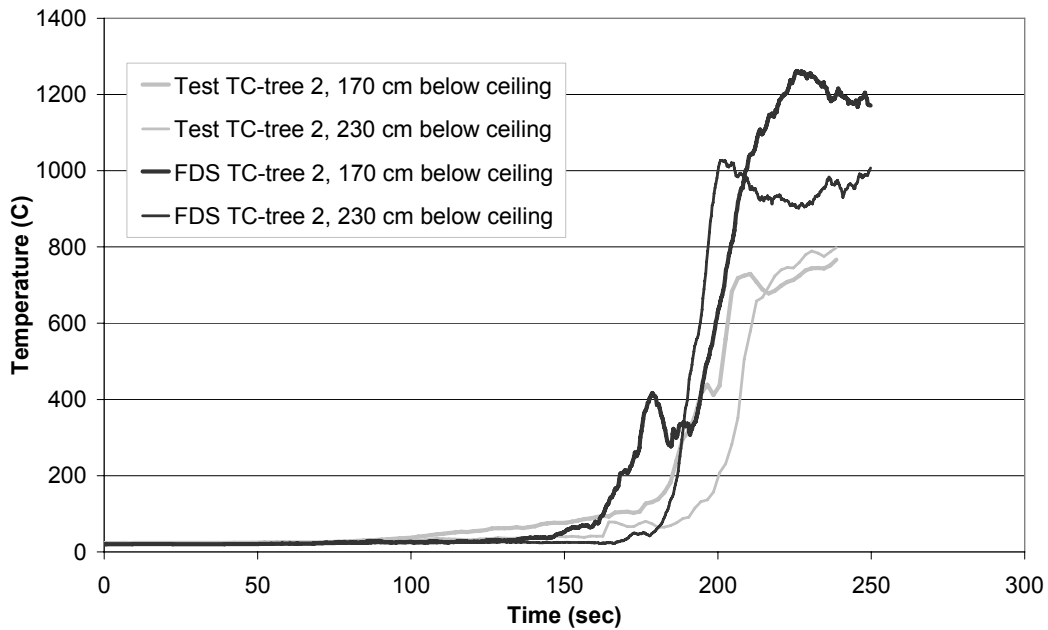


Figure 46 Experimental (grey) and FDS (black) results for temperatures measured by TC-tree 2 (see Figure 4) 170 – 230 cm below the ceiling.

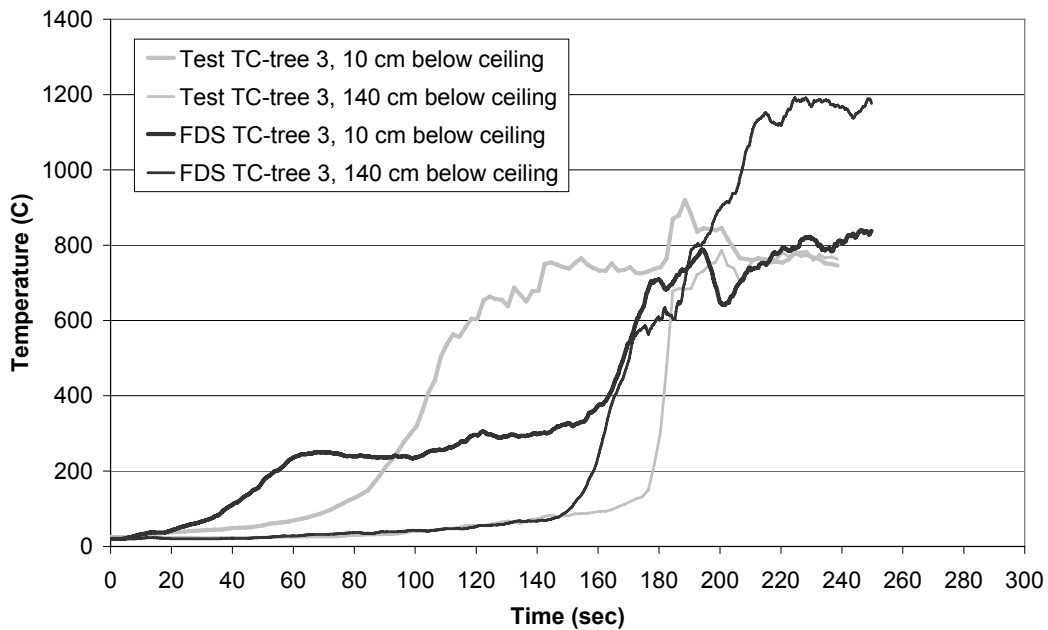


Figure 47 Experimental (grey) and FDS (black) results for temperatures measured by TC-tree 3 (see Figure 4) 10 – 140 cm below the ceiling.

6.2.1 Grid size dependency

The extra simulations with the FDS model were conducted using the grid cell sizes 25, 33 and 75 mm respectively, instead of the 50 mm originally used. The generated HRR in the model is highly dependent on the grid cell size as is evident in Figure 48. The reason is the grid cell size sensitivity of some of the sub-models involved in flame spread, and empirical constants that are more suitable to a certain relation of the grid cell size relative

the fire size. FDS's sensitivity to the mesh is a well known and frequently discussed subject, as is found in the FDS Users Manual [26] and at the FDS discussion forum [28].

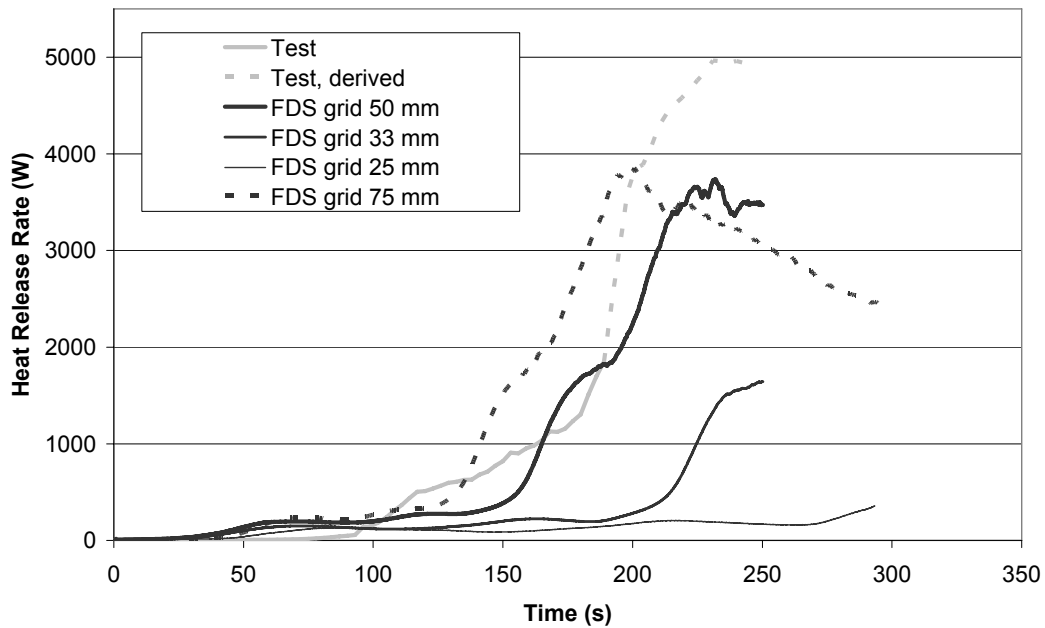


Figure 48 Influence of the grid cell size on the HRR generated in the model.

The grid size dependency shown in Figure 48 is a major drawback for flame spread simulations using FDS. However, since the model has been successfully validated for a 50 mm grid size it is reasonable to assume that the results would still be valid as long as the geometry and the materials do not differ significantly from the configuration of the compartment in the full scale test.

7 Other methods

In this report t^2 curves without input from small scale tests and superposition as well as field modeling with input from small scale tests were used to replicate, at least qualitatively, the fire development of a full-scale test. Other methods could also be considered but, as will be discussed below, these are probably less adequate for enclosures that are furnished in such a complex way as train compartments. Two possible methods are presented below, i.e., two-zone models and strict correlation analysis using the software Conetools.

7.1 Two-zone models

In two-zone models the compartment is typically divided into a few different zones such as a hot upper smoke gas layer, a colder lower layer, fire, and plume. In each layer the gas temperature is assumed to be uniform and there is a discrete horizontal layer between the upper and lower layer. Examples of software where two-zone models are implemented are Branzfire [29] and CFAST [30]. Although more or less advanced models for flame spread are implemented in these software packages these are valid for flame spread of surface linings. Since in the case of a train compartment the furniture, especially the seats, are the most important items for the pre-flashover dynamics it is difficult to use two-zone models for train design fires in a meaningful way. Fire load from burning objects such as seats can be prescribed but it is necessary to know in advance how these heat release curves look like and when the objects will ignite. This is much the same as superposition of HRR curves as was described in section 5. However, if the point of interest is to see how different wall and ceiling linings, or depletion of oxygen, affect the total fire performance two-zone models could be useful. Their main advantage is that they are much simpler and numerically less time consuming than field models such as FDS5.

7.2 ConeTools

Another approach for predicting large scale fire spread is to conduct a correlations analysis between small scale and large scale tests. ConeTools [31] uses test results from the cone calorimeter as input and produces predictions for heat release rates in the ISO 9705 room. This is a powerful method but the software as such is only optimized for the ISO 9705 room geometry and a 100 kW burner in the inner right corner of the room, without any other objects in the room than the surface linings. This is obviously not the same conditions as those prevailing in a train compartment with a complex furnishing. Therefore the use of correlations methods such as ConeTools has not been considered in this report.

8 Discussions and conclusions

Three methods for determining design fires have been investigated: pre-flashover t^2 fires, superposition of HRR curves from small scale tests, and field modelling using FDS5 and material parameters from small scale tests as input.

Pre-flashover t^2 fires gives good agreement with the full scale test until the time of flashover, if a fast growth rate is assumed. The expression for the heat release rate would then be $HRR = 10^6 \cdot t^2 / 150^2$, with t in seconds and HRR in Watts. After flashover the HRR is vastly underestimated. The large discrepancy between the t^2 fire and the full scale test after flashover is not surprising given the fact the former were conceived for pre-flashover fires. If a ultra fast growth rate is assumed, with a characteristic time scale of 75 s instead of 150 s, the dynamics is better reproduced if the start of the fire growth is shifted to the point where, in the full scale experiment, HRR has reached 50 kW. This is, however, a relatively contrived way of defining the t^2 curve since the time when 50 kW has been reached is *a priori* not known, unless full scale experiments are performed, something which this method aims to avoid.

Superpositioning of HRR curves from small scale tests can be performed in many different ways. In this report the first method was to add HRR curves for the seats using the knowledge of the sequence of ignition times from the full scale compartment test (Example 1). This exercise was followed by two simple ways to proceed with no assumptions concerning when the different materials ignite. The absolutely simplest method is to assume the seats are the governing factor, make a test of one seat in the furniture calorimeter and then multiply the obtained HRR curve with the number of seats in the compartment (Example 2). This gives a HRR curve that grows faster than the full scale experiment in the early phase but then underestimates the HRR at the point of flashover. Another method tested was to simply assume that all materials in the entire compartment will behave with the same dynamics as when tested under 50 kW/m² heat irradiation in the cone calorimeter, with the exception of the seats where data from the test in the furniture calorimeter was used (Example 3). This gives an even faster initial growth of the fire but the HRR at flashover is reproduced better. One observation is that the superposition methodology never manages to reproduce the high HRR observed in the full scale experiment after flashover. The most likely explanation for this is that the heat transfer by radiation and convection is much higher in the compartment after flashover than it is in the cone calorimeter with 50 kW/m² irradiation. Using more intelligent assumptions, about the ignition time of the different parts and materials in the compartment, would improve the agreement with the full scale test. Such improved assumptions could for example be worked out by using FDS5 to simulate radiation levels in the compartment as a function of time.

Field modelling with FDS5 did reproduce the full scale results to a satisfying degree. However, it should be remembered that this was done for a certain grid size, 5 cm, and after tuning the conductivity of the seat material to a level that gave the desired results. The latter reservation is surmountable since the selected conductivity is within the limits that can be expected for PUR-foam. The grid sensitivity is a bigger problem since it means that a refined grid, which normally would result in a more accurate computation, actually would produce results that substantially deviate from the full scale test. This is a typical problem for field modelling of flame spread and the basic message is to avoid this type of simulations. However, since the model in this case has been successfully validated against the result from the full-scale experiment it can be assumed that moderate deviations from the compartment configuration, geometry-wise and material-wise, would still give acceptable results if the 5 cm grid size is kept.

Summarizing the finding in this report it has been found that all three methods are useful if the studied compartment does not deviate too much from the one studied here. The method of choice would then be to use a pre-flashover t^2 curve with fast growth rate since this is the simplest method. If the type of compartment is considerably different, such as a bus for example, it seems appropriate to use the superposition method where the HRR curves of the different materials in the vehicle are summarized. In order to estimate ignition times FDS5 could be used to simulate the heat flux levels at different times and at different positions of the bus for a predefined fire size. This can be recommended despite the drawbacks of FDS5 mentioned above since it is well known that the flow dynamics of the hot gases is well described by FDS5, as opposed to flame spread. Finally if post-flashover HRR information is needed FDS5 seems to be the only possible choice since this method takes oxygen depletion into consideration. Again, if the compartment is relatively similar to the compartment tested in this study the confidence in the obtained design fire is relatively high. If the compartment is fundamentally different any attempt to obtain a design fire for post flashover conditions by only performing small scale tests are subject to great difficulties and a new full-scale tests is advisable.

It should be noted that the models in this report are discussed as tools to be used when constructing a design fire without any consideration of their pros and cons when used for performing the subsequent fire engineering analysis of the design fire scenario. Table 6 below summarized the findings.

Table 6 Recommendations for methods in the development of design fires.

	Pre-flashover	Post-flashover
Similar compartment	fast t^2 fire	Existing validated FDS model + small-scale tests as input to FDS
Different compartment	superposition of HRR curves + small scale tests to obtain HRR curves (+ gas phase FDS)	full-scale test

Appendix A: Radiation measurements from the full scale test

The irradiation measured with the two Schmidt-Boelter type instruments (Medtherm 64-1-18 and Medtherm 64-2-18) are shown in Figure 49 below. In order to not damage the instruments they were removed from the compartment 185 s after ignition.

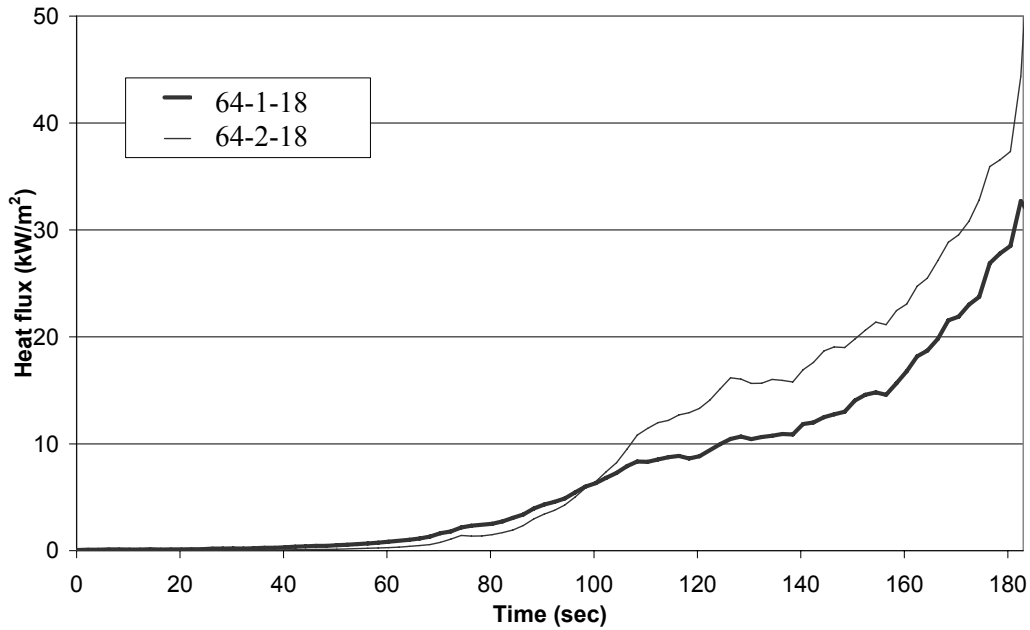


Figure 49 Irradiation levels on instruments Medtherm 64-1-18 and 64-2-18. Medtherm 64-1-18 is facing to the right while Medtherm 64-2-18 is facing upwards. The positions of the calorimeters are shown in Figure 7.

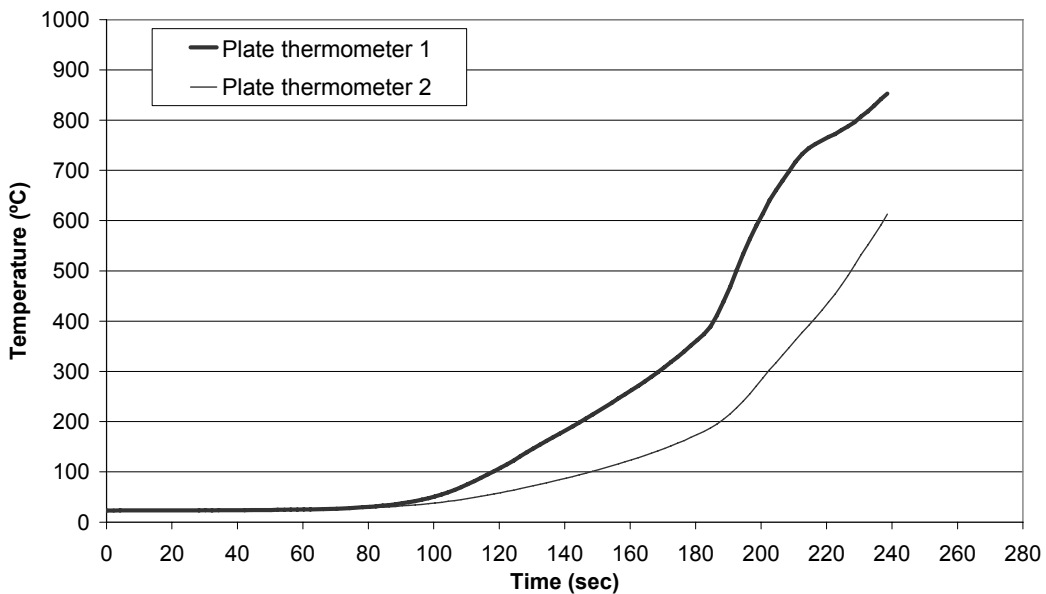


Figure 50 Temperature measured with the plate thermometers. Plate thermometer 1 is facing to the right while plate thermometer 2 is facing upwards. The positions of the plate thermometers are shown in Figure 7.

Appendix B: Data from the Small scale tests of seat, table, and lining materials

8.1 Seat material

8.1.1 Products

Seat material (PUR foam with fabric on top)

8.1.2 Test specification

Irradiance level: 35, 50, and 75 kW/m².

Calibration constant (C): 0.043015 m^{1/2} g^{1/2} K^{1/2}.

Orientation: Horizontal.

Backing: No other than the non-combustible required in the standard.

Fastening: The product was loosely put on the backing.

Note The retainer frame was used.

8.1.3 Test results

Property	Name of variable	Name of		
		35 kW/m ²	50 kW/m ²	75 kW/m ²
Flashing (min:s)	t _{flash}	-	-	-
Ignition (min:s)	t _{ign}	00:14	00:11	00:03
All flaming ceased (min:s)	t _{ext}	10:00	10:21	07:03
Test time (min:s)	t _{test}	10:00	12:21	09:03
Heat release rate (kW/m ²)	q	See figure 1		
Peak heat release rate (kW/m ²)	q _{max}	284	342	444
Average heat release, 3 min (kW/m ²)	q ₁₈₀	95	124	174
Average heat release, 5 min (kW/m ²)	q ₃₀₀	85	123	180
Total heat produced (MJ/m ²)	THR	58.6	69.2	71.8
Smoke production rate (m ² /m ² s)	SPR	See figure 2		
Peak smoke production (m ² /m ² s)	SPR _{max}	8.98	10.49	15.24
Total smoke production over the non-flaming phase (m ² /m ²)	TSP _{nonfl}	2.9	0.9	0.0
Total smoke production over the flaming phase (m ² /m ²)	TSP _{fl}	617.6	1064.9	1444.2
Total smoke production (m ² /m ²)	TSP	621	1066	1444
Sample mass before test (g)	M ₀	38.9	38.1	38.4
Sample mass at sustained flaming (g)	M _s	39.2	37.9	38.5
Sample mass after test (g)	M _f	11.4	5.9	4.4
Average mass loss rate (g/m ² s)	MLR _{ign-end}	5.2	4.9	7.1
Average mass loss rate (g/m ² s)	MLR ₁₀₋₉₀	4.9	6.3	9.5
Total mass loss (g/m ²)	TML	3153	3619	3856
Effective heat of combustion (MJ/kg)	DH _c	18.6	19.1	18.6
Specific smoke production (m ² /kg)	SEA	197	294	375
Max average rate of heat emission (kW/m ²)	MARHE	154.0	195.3	302.3
Volume flow in exhaust duct (l/s)	V	24	24	24

8.1.4 Graphs of heat release rate and smoke production rate

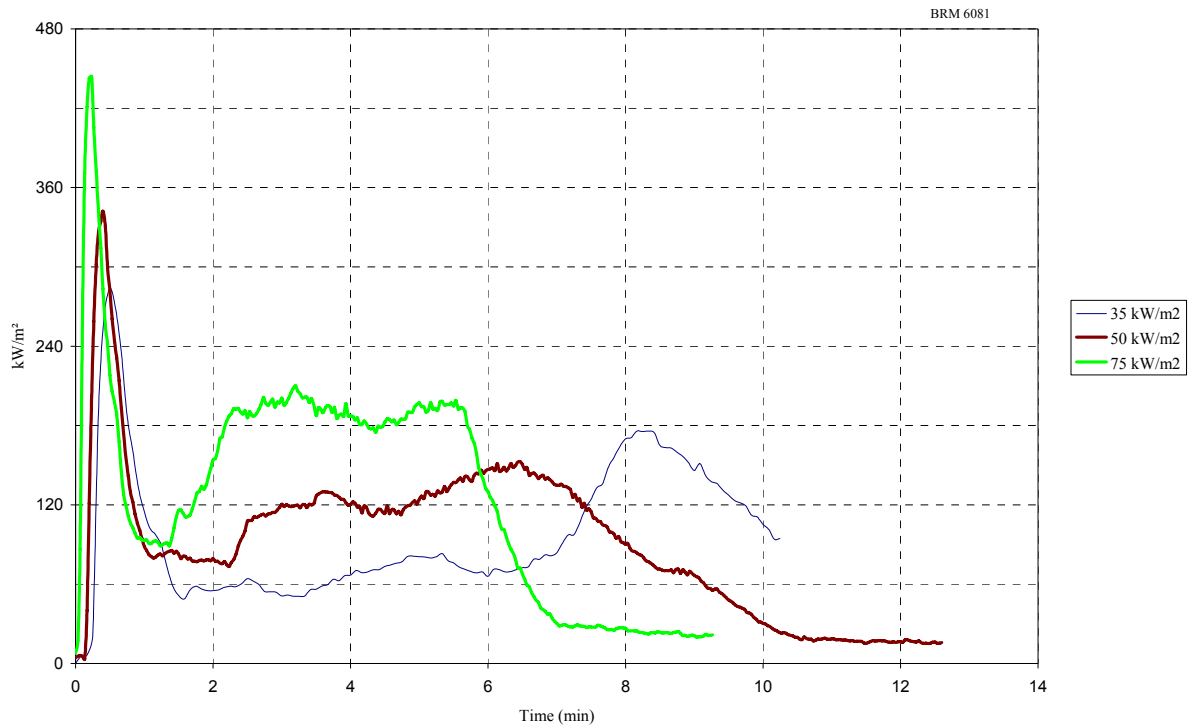


Figure 1 Heat release rate for seat material.

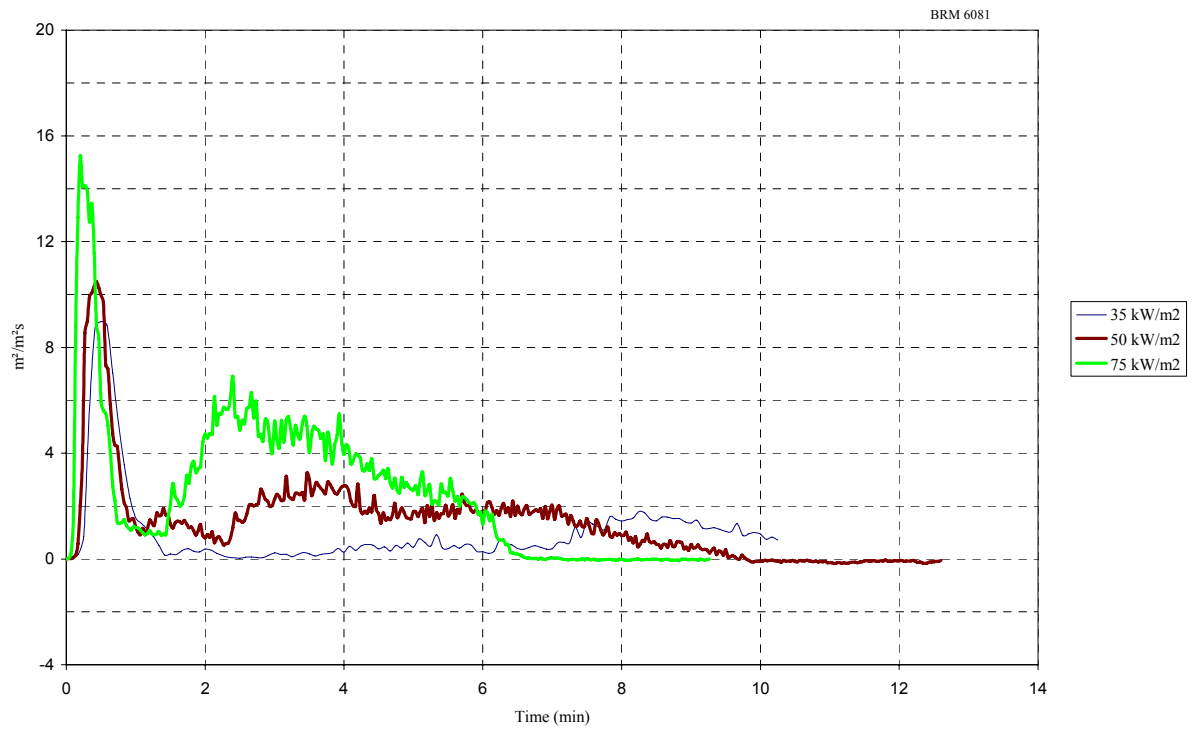


Figure 2 Smoke production rate for seat material.

8.1.5 Measured data

Thickness 50 mm.
Density 77 kg/m³.

8.1.6 Conditioning

Temperature (23 ± 2) °C.
Relative humidity (50 ± 5) %.

8.1.7 Date of test

October 8 and 9, 2008.

8.2 Metal laminate

8.2.1 Products

1.6 mm metal laminate on 18 mm plywood

8.2.2 Test specification

Irradiance level:	35, 50, and 75 kW/m ² .
Calibration constant (C):	0.043015 m ^{1/2} g ^{1/2} K ^{1/2} .
Orientation:	Horizontal.
Backing:	No other than the non-combustible required in the standard.
Fastening:	The product was loosely put on the backing.
Note	The retainer frame was used.

8.2.3 Test results

Property	Name of variable	35 kW/m ² NI, *	50 kW/m ²	75 kW/m ²
Flashing (min:s)	t _{flash}	-	-	-
Ignition (min:s)	t _{ign}	-	01:17	00:46
All flaming ceased (min:s)	t _{ext}	-	02:10	00:00
Test time (min:s)	t _{test}	10:00	03:50	10:00
Heat release rate (kW/m ²)	q	See figure 1		
Peak heat release rate (kW/m ²)	q _{max}	9	58	157
Average heat release, 3 min (kW/m ²)	q ₁₈₀	-	16	70
Average heat release, 5 min (kW/m ²)	q ₃₀₀	-	10	66
Total heat produced (MJ/m ²)	THR	0.9	3.2	45.3
Smoke production rate (m ² /m ² s)	SPR	See figure 2		
Peak smoke production (m ² /m ² s)	SPR _{max}	1.44	7.71	6.89
Total smoke production over the non-flaming phase (m ² /m ²)	TSP _{nonfl}	-	138.0	-
Total smoke production over the flaming phase (m ² /m ²)	TSP _{fl}	-	15.2	-
Total smoke production (m ² /m ²)	TSP	0	153	0
Sample mass before test (g)	M ₀	130.8	122.7	128.5
Sample mass at sustained flaming (g)	M _s	-	118.7	-
Sample mass after test (g)	M _f	118.7	114.4	78.5
Average mass loss rate (g/m ² s)	MLR _{ign-end}	-	3.3	-
Average mass loss rate (g/m ² s)	MLR ₁₀₋₉₀	2.4	2.9	9.9
Total mass loss (g/m ²)	TML	-	479	5293
Effective heat of combustion (MJ/kg)	DH _c	-	6.6	8.6
Specific smoke production (m ² /kg)	SEA	-	320	0
Max average rate of heat emission (kW/m ²)	MARHE	6.8	17.2	75.6
Volume flow in exhaust duct (l/s)	V	24	24	24

NI = no ignition, * No heat release data is given since the specimen did not ignite.

8.2.4 Graphs of heat release rate and smoke production rate

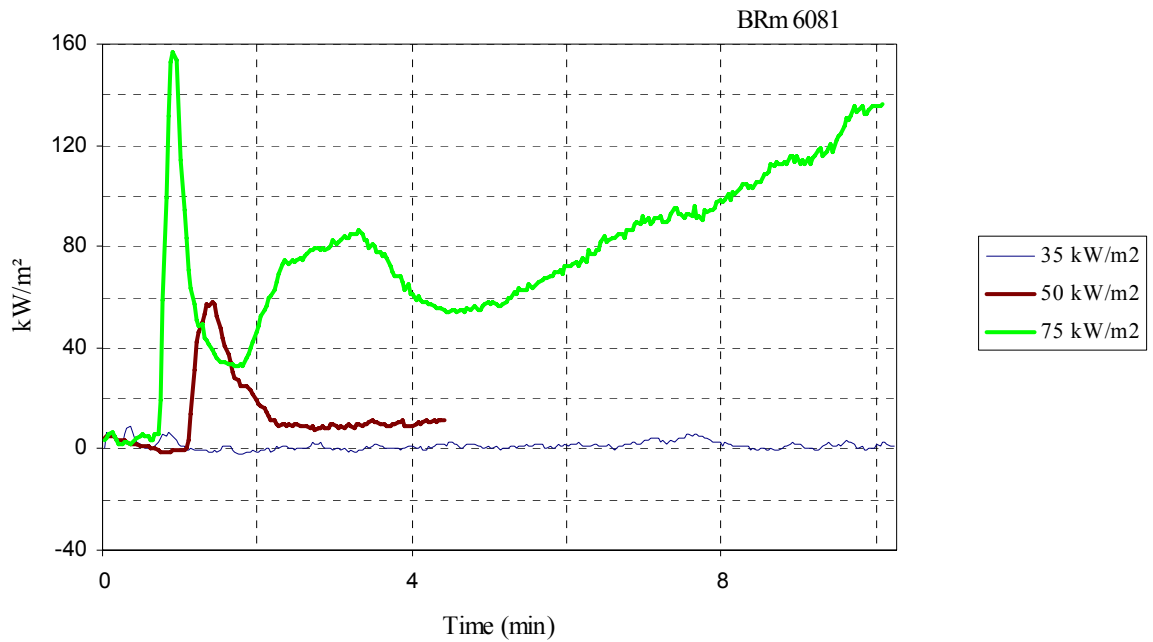


Figure 1 Heat release rate for metal laminate on plywood.

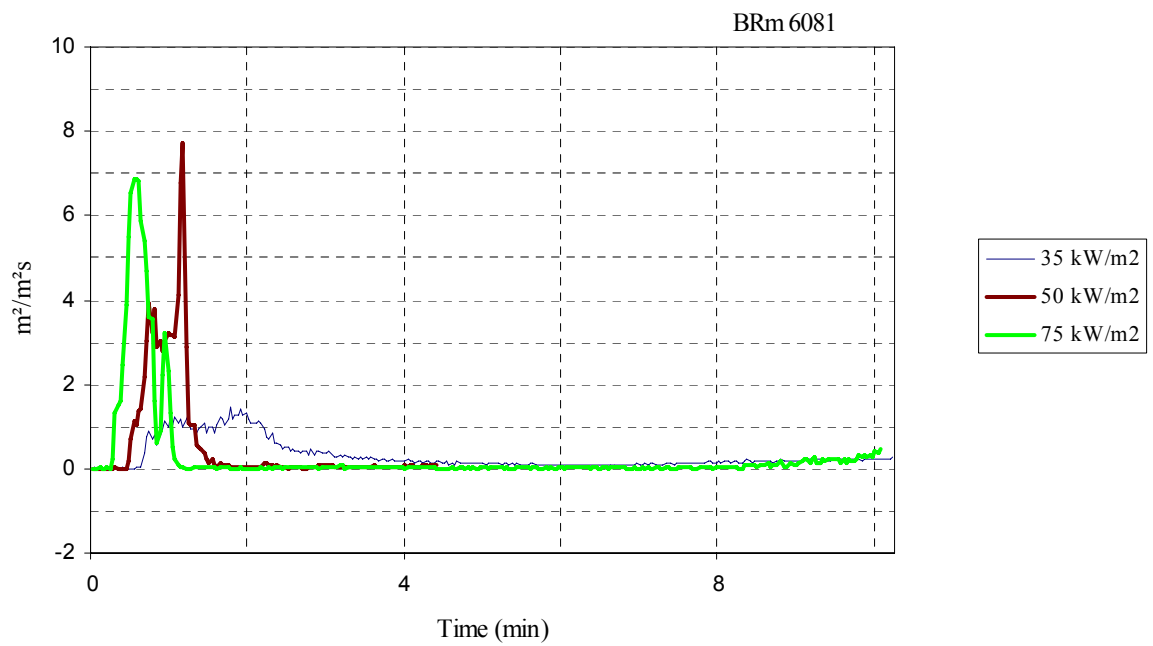


Figure 2 Smoke production rate for for metal laminate on plywood.

8.2.5 Measured data

Thickness 20 mm.
Density 648 kg/m³.

8.2.6 Conditioning

Temperature (23 ± 2) °C.
Relative humidity (50 ± 5) %.

8.2.7 Date of test

October 8 and 9, 2008.

8.3 HPL laminate

8.3.1 Products

1 mm HPL laminate on 18 mm plywood

8.3.2 Test specification

Irradiance level:	35, 50, and 75 kW/m ² .
Calibration constant (C):	0.043015 m ^{1/2} g ^{1/2} K ^{1/2} .
Orientation:	Horizontal
Backing:	No other than the non-combustible required in the standard.
Fastening:	The product was loosely put on the backing.
Note	The retainer frame was used.

8.3.3 Test results

Property	Name of variable	Name of		
		35 kW/m ²	50 kW/m ²	75 kW/m ²
Flashing (min:s)	t _{flash}	-	-	-
Ignition (min:s)	t _{ign}	09:35	01:50	00:14
All flaming ceased (min:s)	t _{ext}	20:00	00:00	00:26
Test time (min:s)	t _{test}	20:00	10:00	05:00
Heat release rate (kW/m ²)	q	See figure 1		
Peak heat release rate (kW/m ²)	q _{max}	133	131	238
Average heat release, 3 min (kW/m ²)	q ₁₈₀	67	113	139
Average heat release, 5 min (kW/m ²)	q ₃₀₀	65	104	122
Total heat produced (MJ/m ²)	THR	53.6	49.5	36.7
Smoke production rate (m ² /m ² s)	SPR	See figure 2		
Peak smoke production (m ² /m ² s)	SPR _{max}	2.18	5.53	5.31
Total smoke production over the non-flaming phase (m ² /m ²)	TSP _{nonfl}	339.0	-	0.1
Total smoke production over the flaming phase (m ² /m ²)	TSP _{fl}	242.3	-	309.2
Total smoke production (m ² /m ²)	TSP	581	0	309
Sample mass before test (g)	M ₀	115.5	100.8	112.4
Sample mass at sustained flaming (g)	M _s	100.3	-	112.4
Sample mass after test (g)	M _f	57.4	54.7	79.7
Average mass loss rate (g/m ² s)	MLR _{ign-end}	7.8	-	12.8
Average mass loss rate (g/m ² s)	MLR ₁₀₋₉₀	7.3	9.3	13.1
Total mass loss (g/m ²)	TML	4849	4506	3703
Effective heat of combustion (MJ/kg)	DH _c	11.0	11.0	9.9
Specific smoke production (m ² /kg)	SEA	120	0	84
Max average rate of heat emission (kW/m ²)	MARHE	44.6	82.6	130.5
Volume flow in exhaust duct (l/s)	V	24	24	24

8.3.4 Graphs of heat release rate and smoke production rate

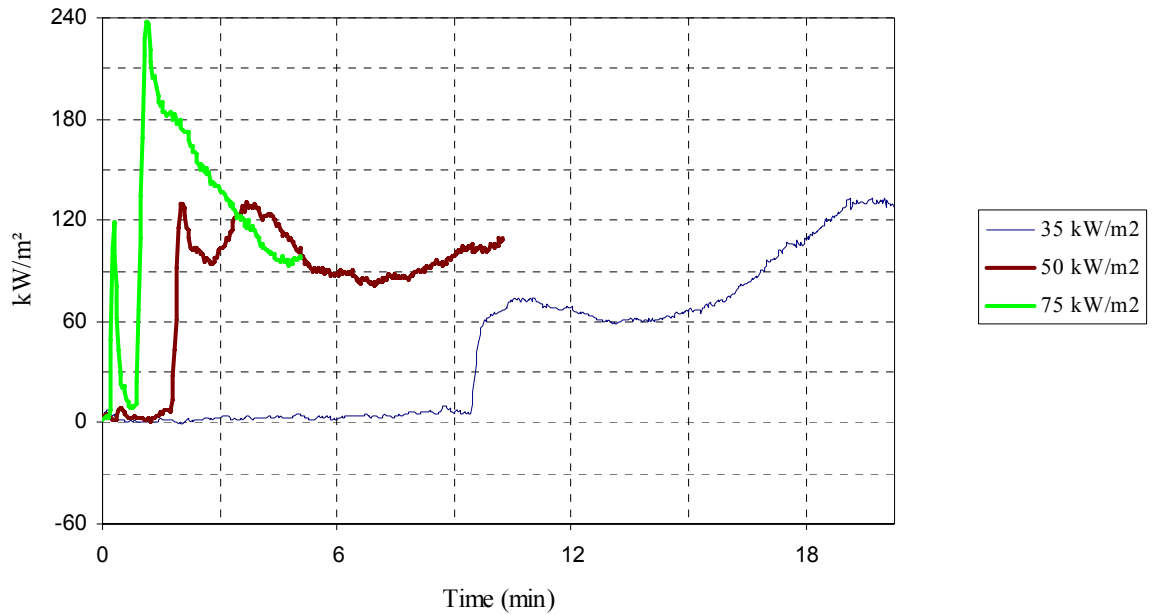


Figure 1 Heat release rate for HPL laminate on plywood.

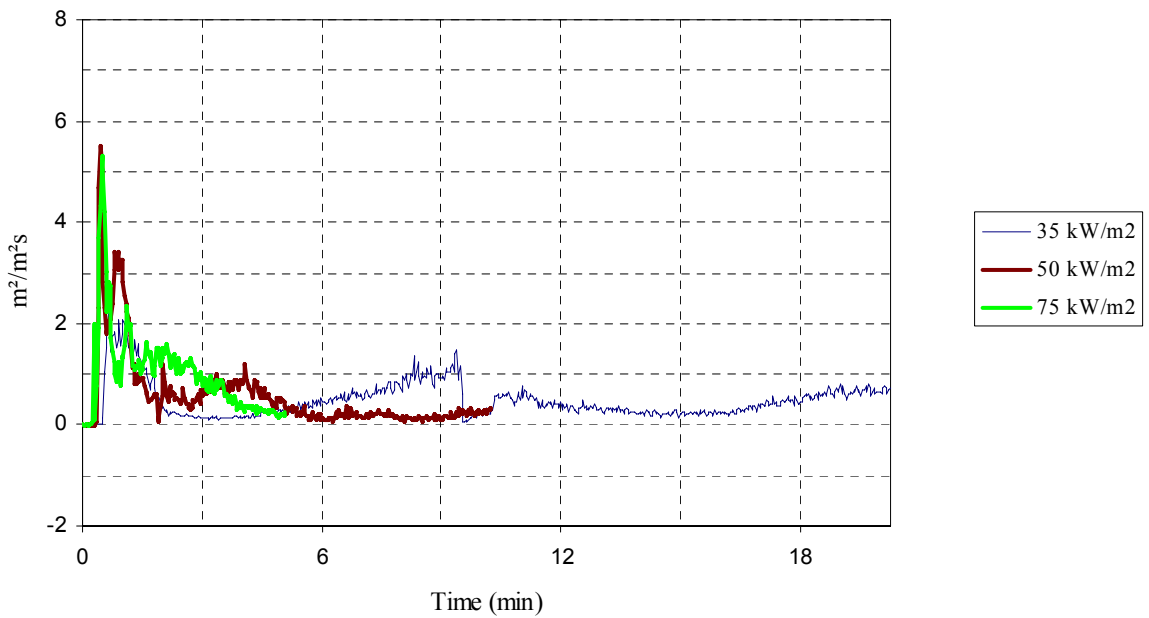


Figure 2 Smoke production rate for HPL laminate on plywood.

8.3.5 Measured data

Thickness 20 mm.
Density 548 kg/m³.

8.3.6 Conditioning

Temperature (23 ± 2) °C.
Relative humidity (50 ± 5) %.

8.3.7 Date of test

October 8 and 9, 2008.

8.4 PVC-carpet

8.4.1 Products

PVC-carpet

8.4.2 Test specification

Irradiance level:	35, 50, and 75 kW/m ² .
Calibration constant (C):	0.043015 m ^{1/2} g ^{1/2} K ^{1/2} .
Orientation:	Horizontal
Backing:	No other than the non-combustible required in the standard.
Fastening:	The product was loosely put on the backing.
Note	The retainer frame was used.

8.4.3 Test results

Property	Name of variable	Name of		
		35 kW/m ²	50 kW/m ²	75 kW/m ²
Flashing (min:s)	t _{flash}	-	-	-
Ignition (min:s)	t _{ign}	00:26	00:12	00:07
All flaming ceased (min:s)	t _{ext}	03:28	02:12	01:47
Test time (min:s)	t _{test}	05:28	04:12	03:47
Heat release rate (kW/m ²)	q	See figure 1		
Peak heat release rate (kW/m ²)	q _{max}	251	284	344
Average heat release, 3 min (kW/m ²)	q ₁₈₀	116	122	122
Average heat release, 5 min (kW/m ²)	q ₃₀₀	75	80	78
Total heat produced (MJ/m ²)	THR	22.8	23.8	23.3
Smoke production rate (m ² /m ² s)	SPR	See figure 2		
Peak smoke production (m ² /m ² s)	SPR _{max}	19.31	29.39	38.84
Total smoke production over the non-flaming phase (m ² /m ²)	TSP _{nonfl}	0.7	0.1	0.1
Total smoke production over the flaming phase (m ² /m ²)	TSP _{fl}	1278.6	1439.2	1582.1
Total smoke production (m ² /m ²)	TSP	1279	1439	1582
Sample mass before test (g)	M ₀	28.9	28.8	28.0
Sample mass at sustained flaming (g)	M _s	28.7	28.8	27.6
Sample mass after test (g)	M _f	11.6	10.7	8.4
Average mass loss rate (g/m ² s)	MLR _{ign-end}	6.5	8.4	9.7
Average mass loss rate (g/m ² s)	MLR ₁₀₋₉₀	13.6	17.8	16.7
Total mass loss (g/m ²)	TML	1932	2048	2176
Effective heat of combustion (MJ/kg)	DH _c	11.8	11.6	10.7
Specific smoke production (m ² /kg)	SEA	662	703	727
Max average rate of heat emission (kW/m ²)	MARHE	139.4	200.6	273.6
Volume flow in exhaust duct (l/s)	V	24	24	24

8.4.4 Graphs of heat release rate and smoke production rate

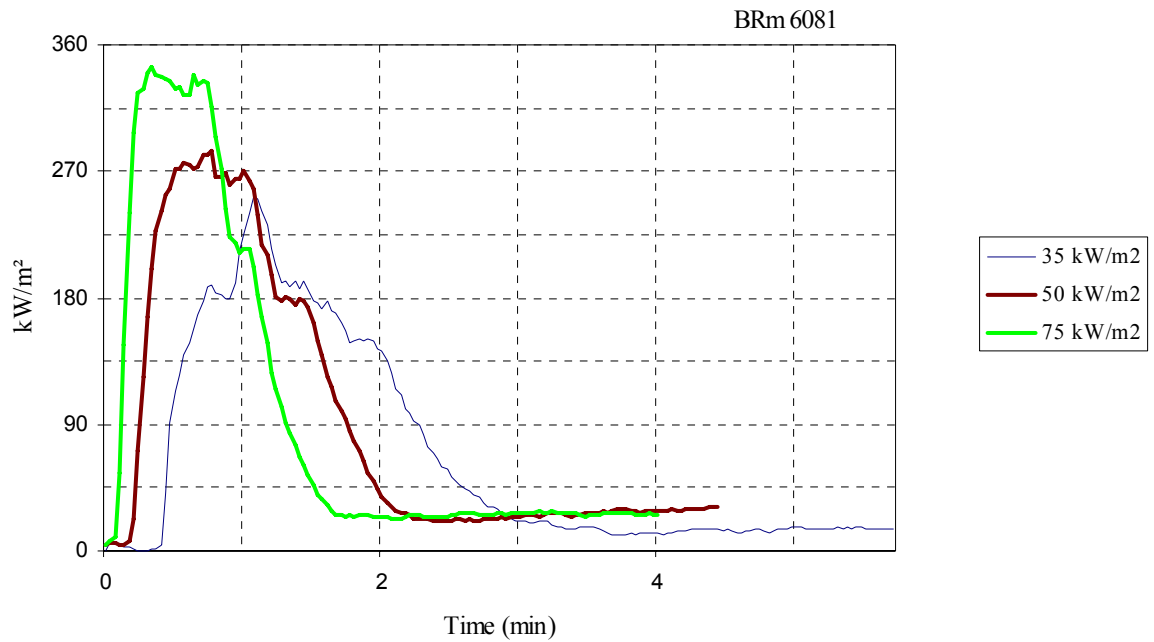


Figure 1 Heat release rate for PVC-carpet.

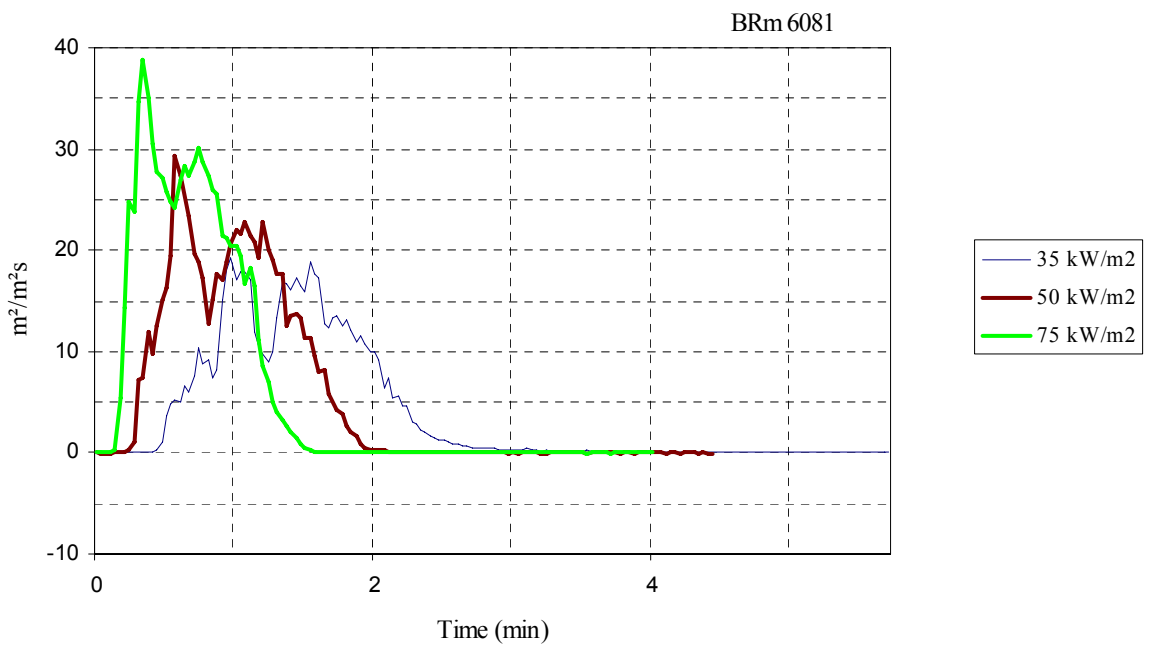


Figure 2 Smoke production rate for PVC-carpet.

8.4.5 Measured data

Thickness 2 mm.
Density 1400 kg/m³.

8.4.6 Conditioning

Temperature (23 ± 2) °C.
Relative humidity (50 ± 5) %.

8.4.7 Date of test

October 9, 2008.

8.5 Wood table

8.5.1 Products

Wood table with HPL laminate on top

8.5.2 Test specification

Irradiance level:	35, 50, and 75 kW/m ² .
Calibration constant (C):	0.043015 m ^{1/2} g ^{1/2} K ^{1/2} .
Orientation:	Horizontal.
Backing:	No other than the non-combustible required in the standard.
Fastening:	The product was loosely put on the backing.
Note	The retainer frame was used.

8.5.3 Test results

Property	Name of variable	Name of		
		35 kW/m ²	50 kW/m ²	75 kW/m ²
Flashing (min:s)	t _{flash}	-	-	-
Ignition (min:s)	t _{ign}	01:41	00:38	00:22
All flaming ceased (min:s)	t _{ext}	00:00	10:00	00:00
Test time (min:s)	t _{test}	10:00	10:00	10:00
Heat release rate (kW/m ²)	q	See figure 1		
Peak heat release rate (kW/m ²)	q _{max}	173	210	364
Average heat release, 3 min (kW/m ²)	q ₁₈₀	83	119	161
Average heat release, 5 min (kW/m ²)	q ₃₀₀	65	99	133
Total heat produced (MJ/m ²)	THR	29.6	46.8	64.5
Smoke production rate (m ² /m ² s)	SPR	See figure 2		
Peak smoke production (m ² /m ² s)	SPR _{max}	2.04	2.98	2.65
Total smoke production over the non-flaming phase (m ² /m ²)	TSP _{nonfl}	-	5.5	-
Total smoke production over the flaming phase (m ² /m ²)	TSP _{fl}	-	106.8	-
Total smoke production (m ² /m ²)	TSP	0	112	0
Sample mass before test (g)	M ₀	181.4	186.0	187.3
Sample mass at sustained flaming (g)	M _s	-	185.3	-
Sample mass after test (g)	M _f	150.5	143.5	129.8
Average mass loss rate (g/m ² s)	MLR _{ign-end}	-	8.5	-
Average mass loss rate (g/m ² s)	MLR ₁₀₋₉₀	6.0	8.1	10.8
Total mass loss (g/m ²)	TML	3176	4735	6470
Effective heat of combustion (MJ/kg)	DH _c	9.3	9.9	10.0
Specific smoke production (m ² /kg)	SEA	0	24	0
Max average rate of heat emission (kW/m ²)	MARHE	64.6	110.0	183.8
Volume flow in exhaust duct (l/s)	V	24	24	24

8.5.4 Graphs of heat release rate and smoke production rate

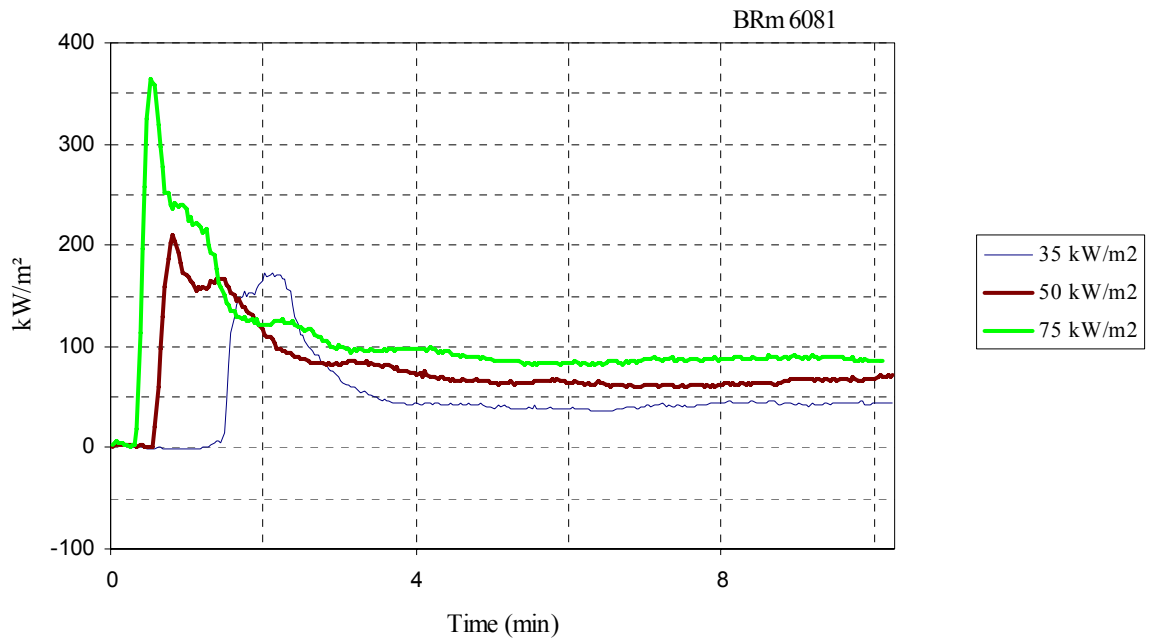


Figure 1 Heat release rate for wood table with HPL laminate on top..

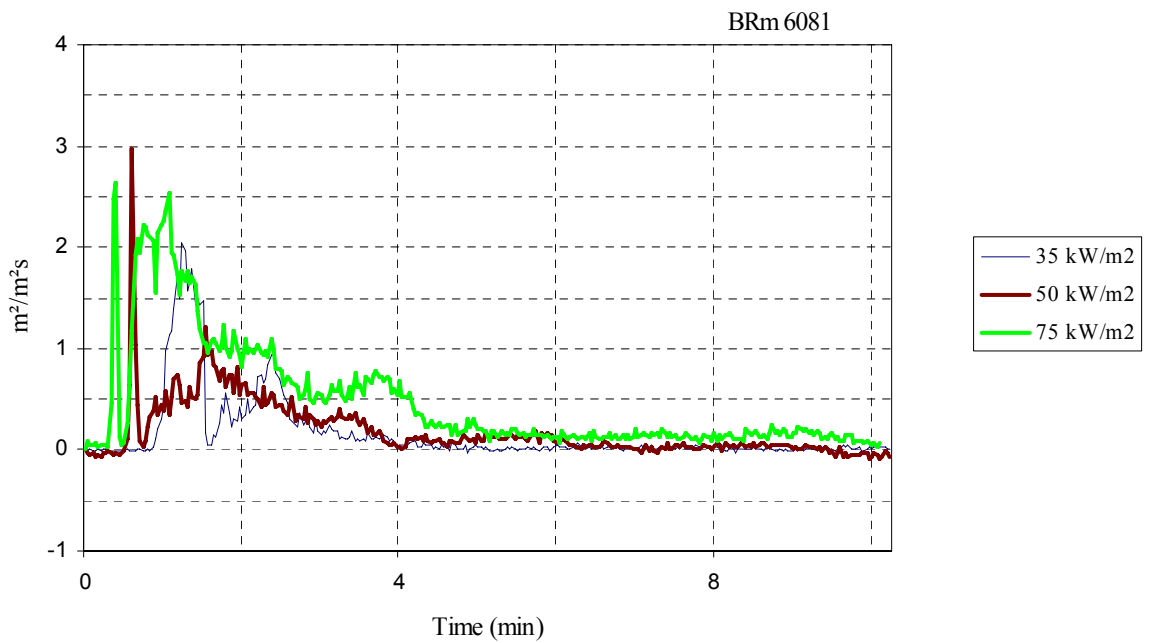


Figure 2 Smoke production rate for wood table with HPL laminate on top.

8.5.5 Measured data

Thickness 30 mm.
Density 616 kg/m³.

8.5.6 Conditioning

Temperature (23 ± 2) °C.
Relative humidity (50 ± 5) %.

8.5.7 Date of test

October 8 and 9, 2009.

8.6 Test results explanation – ISO 5660

Parameter	Explanation
Test start	The test specimen is subjected to the irradiance and the clock is started.
t_{flash}	Time from test start until flames with shorter duration than 1 s.
t_{ign}	Time from test start until sustained flaming with duration more than 10 s.
T_{ext}	Time from test start until the flames have died out.
End of test	Defined as the time when both, the product has been extinguished for 2 minutes, and the mass loss is less than 150 g/m ² during 1 minute.
T_{test}	Test time. From test start until end of test.
q_{max}	Peak heat release rate during the entire test.
q_{180}	Average heat release rate during 3 minutes from ignition. If the test is terminated before, the heat release rate is taken as 0 from the end of test.
q_{300}	Average heat release rate during 5 minutes from ignition. If the test is terminated before, the heat release rate is taken as 0 from the end of test.
THR	Total Heat Released from test start until end of test.
SPR_{max}	Peak Smoke Production Rate from test start until end of test.
TSP	Total Smoke Produced from test start until end of test.
M_0	Mass of specimen.
M_s	Mass of specimen at sustained flaming.
M_f	Mass of specimen at the end of the test.
$\text{MLR}_{\text{ign-end}}$	Mass Loss Rate. Average mass loss rate from ignition until end of test.
MLR_{10-90}	Mass Loss Rate. Average mass loss rate between 10% and 90% of mass loss.
TML	Total mass loss from ignition until end of test.
ΔH_c	Effective heat of combustion calculated as the ratio between total energy released and total mass loss calculated from ignition until end of test.
SEA	Specific Extinction Area defined as the ratio between total smoke released and total mass loss calculated from test start until end of test.
MARHE	Maximum Average Rate of Heat Emission defined as the maximum of the function (cumulative heat release between $t = 0$ and $\text{time} = t$) divided by ($\text{time} = t$).
V	Volume flow rate in exhaust duct. Average during the test.

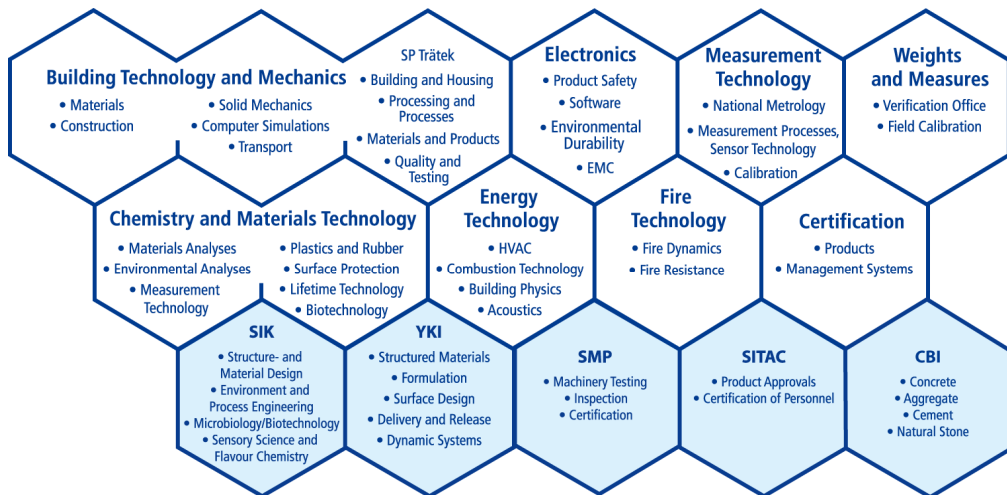
References

1. ISO/TS 16733, *Fire Safety Engineering - Selection of Design Fire Scenarios and Design Fires*, 2006.
2. *Fires in transport tunnels - Report on full-scale tests*, EUREKA-project EU 499:FIRETUNE, 1995.
3. Haukur Ingason and Anders Lönnermark, *Brandbelastning och brandscenarier för järnvägstunnlar*, SP Rapport 2004:30, 2004.
4. Briggs et al, *Work package 8.1: Real-scale reaction to fire tests on structural products used on European trains*, FIRESTARR project, 2001.
5. N. White, V. Dowling, and J. Barnett. *Full-scale Experiment on a Typical Passenger Train*. in *Fire Safety Science - Proceedings of the 8th International Symposium*, 2005.
6. R. Peacock and et al, *Fire Safety of Passenger Trains, Phase III: Evaluation of Fire Hazard Analysis Using Full-Scale Passenger Rail Car Tests*, NISTIR 6563, 2004.
7. R. Peacock and E. Braun, *Fire Safety of Passenger Trains; Phase I: Material Evaluation (Cone Calorimeter)*, NISTIR 6132, 1999.
8. R. Peacock and et al, *Fire Safety of Passenger Trains; Phase II: Application of Fire Hazard Analysis Techniques*, NISTIR 6525, 2002.
9. ISO/TR 13387-2 *Fire safety engineering - Part 2: Design fire scenarios and design fires*.
10. <http://www.jarnvag.net/vagnguide/BF4.asp>.
11. Ulf Wickström, *The plate thermometer - a simple instrument for reaching harmonized fire resistance tests*. *Fire Technology*, 1994. **30**(2): p. 195-208.
12. *ISO 9705 Fire tests - Full-scale room test for surface products*, 1993.
13. *Final draft prCEN/TS 45545-2 Railway applications - Fire protection of railway vehicles - Part 2: Requirements for fire behaviour of materials and components*, CEN, February 2008.
14. *ISO 5660-1:2002 Reaction-to-fire tests -- Heat release, smoke production and mass loss rate - Part 1: Heat release rate (cone calorimeter method)*, 2002.
15. Vytenis Babrauskas, *Ignition Handbook: Principles and Application to Fire Safety Engineering, Fire Investigation, Risk Management and Forensic Science*. 2003: Fire Science Publishers.
16. M. L. Janssens, *Fundamental Thermophysical Characteristics of Wood and Their Role in Enclosure Fire Growth*. 1991, *Fundamental Thermophysical Characteristics of Wood and Their Role in Enclosure Fire Growth*, University of Gent: Gent.
17. M. L. Janssens, *Piloted Ignition of Wood: A Review*. *Fire and Materials*, 1991. **15**: p. 151-167.
18. <http://people.bath.ac.uk/absmaw/BEnv1/properties.pdf>.
19. http://en.wikipedia.org/wiki/Polyethylene_terephthalate.
20. *Appendix B Property Data*, in *The SFPA Handbook of Fire Protection Engineering*, P.J. DiNunno, Editor. 1995, NFPA.
21. http://www.engineeringtoolbox.com/specific-heat-solids-d_154.html. [cited.
22. <http://webbook.nist.gov/cgi/cbook.cgi?ID=C108952&Units=SI&Mask=2#Thermo-Condensed>.
23. <http://www.goodfellow.com/E/Polyvinylchloride-Unplasticised.html>.
24. ISO/TR 13387.2:1999 *Fire safety engineering - Part 2: Design fire scenarios and design fires*, 1999.
25. *CBUF Fire Safety of Upholstered Furniture-the final report of the CBUF research programme. Report EUR 16477 EN.*, ed. B. Sundström.

26. K. McGrattan, B. Klein, S. Hostikka, and J. Floyd, *Fire Dynamics Simulator (Version 5) User's Guide*, 2007.
27. J. Söderbom, *EUREFIC - Large Scale Test according to ISO DIS 9705, SP Report 1991:27*, 1991.
28. <http://groups.google.com/group/fds-smv>.
29. C. A. Wade, *A User's Guide to BRANZFIRE 2004*.
30. R. D. Peacock, W. Jones, P. A. Reneke, and G. P. Forney, *CFAST - Consolidated Model of Fire Growth and Smoke Transport (Version 6) User's Guide*. 2005, NIST.
31. <http://www.sp.se/sv/index/services/calculations/conetools/Sidor/default.aspx>.

SP Technical Research Institute of Sweden develops and transfers technology for improving competitiveness and quality in industry, and for safety, conservation of resources and good environment in society as a whole. With Sweden's widest and most sophisticated range of equipment and expertise for technical investigation, measurement, testing and certification, we perform research and development in close liaison with universities, institutes of technology and international partners.

SP is a EU-notified body and accredited test laboratory. Our headquarters are in Borås, in the west part of Sweden.



SP is organised into eight technology units and five subsidiaries



SP Technical Research Institute of Sweden

Box 857, SE-501 15 BORÅS, SWEDEN

Telephone: +46 10 516 50 00, Telefax: +46 33 13 55 02

E-mail: info@sp.se, Internet: www.sp.se

www.sp.se

Fire Technology

SP Report 2009:08

ISBN 91-7848-978-91-85829-79-

8

ISSN 0284-5172